AN ABSTRACT OF THE THESIS OF

DONALD FREDERICK KEENE for the MASTER OF SCIENCE
(Name) (Degree)

in OCEANOGRAPHY presented on May 10, 1971
(Major) (Date)

Title: A PHYSICAL OCEANOGRAPHIC STUDY OF THE NEARSHORE ZONE AT NEWPORT, OREGON

Abstract approved: Redacted for Privacy
Victor T. Neal

The nearshore zone at Newport, Oregon was studied during the period September, 1968 to August, 1969. Particular emphasis was placed on those physical factors affecting the distribution of pulp mill wastes discharged within the study area (referred to as Yaquina Bight in this thesis). Temperatures and seawater samples were obtained from a small boat. Nearshore and longshore currents were measured from a light aircraft using dye markers and drift bottles, respectively. Winds, waves and tides were measured from shore stations. This thesis describes the waters of the bight throughout the year and how they are affected by the effluent of the pulp mill and by seasonal oceanic and local conditions.

The waters within Yaquina bight reflect the large scale seasonal oceanic conditions which occur off the Oregon coast, i.e., the summer upwelling season and the winter Davidson current season. On a smaller scale the waters of the bight are influenced by the pulp mill

effluent. The effluent mixes rapidly with seawater and the mixture is generally colder, less saline and less dense than the surrounding surface waters. The dissolved oxygen content of the mixture is also lower than the surrounding seawater. The analyses of different effluent-seawater dilutions indicated that the low oxygen content is not caused by chemical reactions of the effluent.

Measurements of current velocity at a depth of two meters were regressed on concurrent measurements of the prevailing wind, waves and tide. The local wind of the hour previous to the time of observation accounted for 56.9% of the variance of the currents flowing in the north-south direction at the outfall station. The wind also accounted for 26.6% of the variance of the east-west flowing currents at the outfall station. Currents at other stations within the bight were also analyzed. The unexplained variance of the currents at the other stations was higher than those at the outfall station.

Deviations between the surface current direction and the current direction at two meters were apparently related to the season and to the wind speed. At wind speeds greater than seven meters per second the angle between the two current directions approached zero. The data did not indicate that the deeper current flowed to the left or the right of the surface current as a function of wind speed. However, during the upwelling season the current at two meters was observed to flow consistently to the left of the surface current.

A Physical Oceanographic Study of the Nearshore Zone at Newport, Oregon

by

Donald Frederick Keene

A THESIS

submitted to

Oregon State University

in partial fulfillment of
the requirements for the
degree of

Master of Science

June 1971

APPROVED:

Redacted for Privacy

Assistant Professor of Oceanography
in charge of major

Redacted for Privacy

Chairman of Department of Oceanography

Redacted for Privacy

Dean of Graduate School

Date thesis is presented 15 May 1971

Typed by Mary Jo Stratton for Donald Frederick Keene

ACKNOWLEDGEMENTS

It is a pleasure to acknowledge the encouragement, enthusiasm and guidance of Dr. Victor Neal. His assistance and friendship have contributed greatly to all phases of this study.

I also appreciate the efforts of Doug Coughenower, formerly of the Oregon State University Marine Science Center at Newport, Oregon for the accurate analysis of salinity and dissolved oxygen for the many sea water samples collected during the research period. Mr. George Ditsworth and Mr. Richard Callaway of the Pacific Northwest Water Laboratory in Corvallis provided wind data during the first half of the project.

I am also indebted to my wife and children for their patience and understanding during the previous two years. Many of their activities have been relinquished for the pursuit of this degree.

This study was partially supported by Federal Water Pollution Control Administration Grant 16-070 EMO.

TABLE OF CONTENTS

LIST OF TABLES

LIST OF FIGURES

A PHYSICAL OCEANOGRAPHIC STUDY OF THE NEARSHORE ZONE AT NEWPORT, OREGON

INTRODUCTION

The rate of construction of industrial waste and municipal sewage outfalls along the Pacific Coast has increased considerably during the last two decades, particularly near high population centers. Oregon has no large cities on the coast but large volumes of pulp mill wastes are disposed of in the ocean.

Prior to an outfall's construction, investigations are conducted to provide the information necessary to calculate dilution rates of an effluent at a given distance from the ocean outfall. These studies are often conducted during short periods of optimum weather conditions. Therefore, interpretation of the data frequently does not provide a satisfactory or complete description of the outfall area.

For a period of nearly one year (September 1968 to August 1969), the Department of Oceanography at Oregon State University conducted a study of the physical factors in the nearshore marine environment at Newport, Oregon, with particular emphasis on those factors affecting the distribution of pulp mill wastes discharged within the study area. The observations included measurements of nearshore currents (those currents seaward of the surf zone), longshore currents (those inside the surf zone), breaker heights, breaker periods, angles of wave approach, water temperatures, salinity, dissolved oxygen, tides,

and local wind. The study area is unique, being somewhat enclosed by Yaquina Head and Yaquina Reef (Figure 1). It is approximately 8.0 km long and 1.6 km wide. Yaquina Reef, about 1.6 km from the beach, runs parallel to the shore, forming a submerged, broken boundary of the area. To the south lies the north jetty of Yaquina Bay, which extends from the beach out to Yaquina Reef. Yaquina Head, a 100 meter high rocky headland, forms the northern boundary. This promontory extends about 1.5 km from the general coastline. The area can be considered as an open bay, and for convenience will be referred to as Yaquina Bight, or the bight.

The purpose of this thesis is twofold. One part is a description of the waters found in the bight throughout the year and how they affect or are affected by the effluent of the pulp mill outfall. The relation of the hydrographic data to seasonal oceanic and local conditions is emphasized. The second part is a statistical study of the advection processes observed in the bight. The contribution and importance of known and suspected current-producing forces are examined by regression analysis. The result is a prediction equation for the observed currents using parameters that are easily obtained. The longshore currents are also examined in a similar manner.

The units of measurement for oceanographic work have been derived from a number of disciplines; subsequently, no simple system has prevailed. All measurements in this study were taken in English

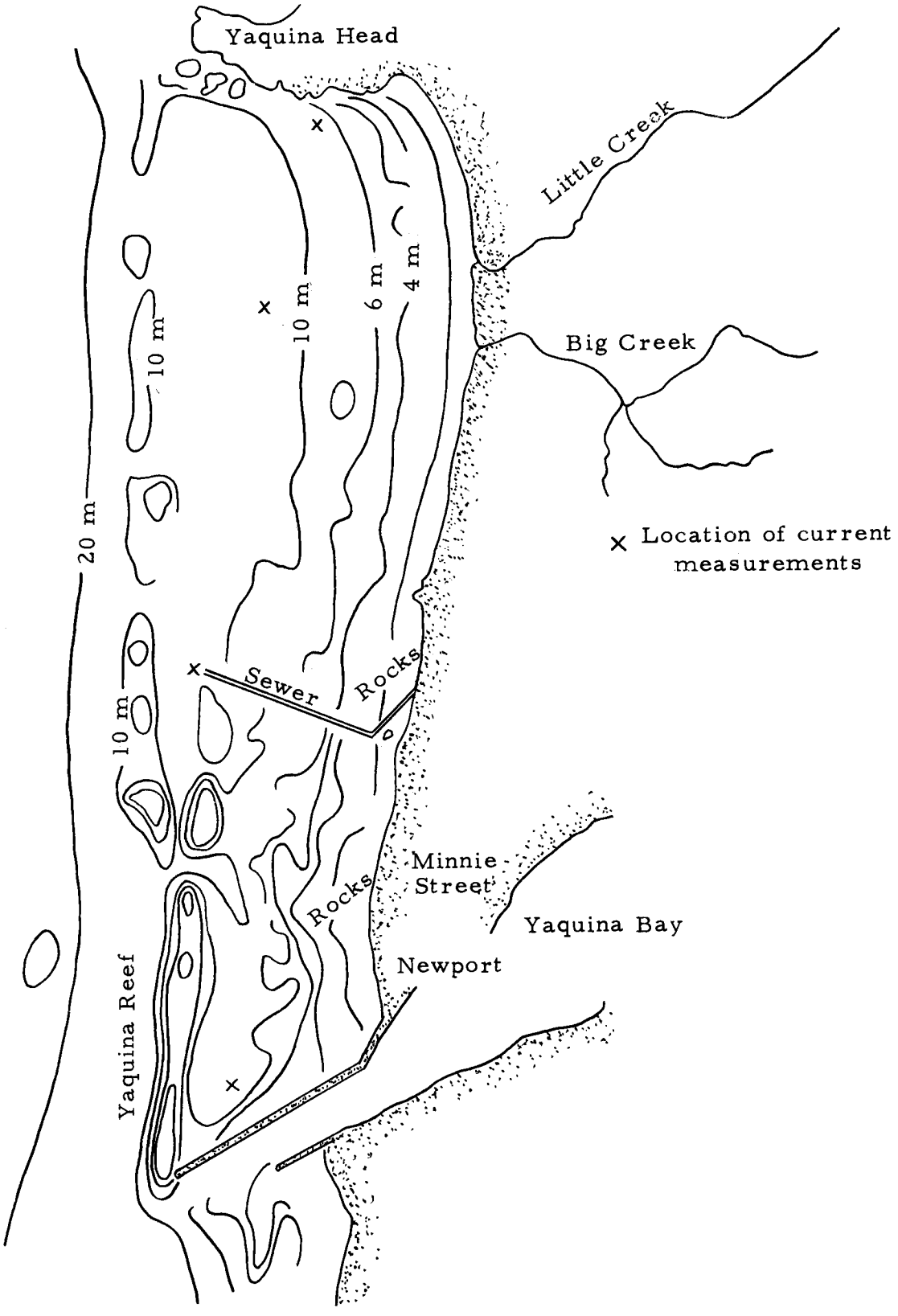

Figure 1. Chart of the nearshore region, Newport, Oregon.

units because all the instruments used indicated English units. These instruments were the navigation charts, aircraft altimeter, wave staffs, wind anemometers, and the tide gauge. Rather than convert each value to the metric system during recording, the values were retained in their original units to avoid confusion and for ease of measurement. However, the results of this study are given in the metric system. Where work is cited from the literature, units are converted into the metric system.

Background

The pulp mill effluent was originally discharged directly into the surf at Newport. Residents objected to the odor as well as the unsightly foam which accumulated on the beach. Therefore, a limited study (Tollefson, 1958) was conducted to determine how these problems could be alleviated. Based on one day of water sampling, Tollefson concluded that physical and chemical testing of the water in the bight was not a satisfactory method for tracing the local water type distribution. He also conducted a one day free-float current study in the immediate vicinity. From the plotted float paths he deduced that an onshore current prevailed. As the floats passed into the breaker zone, a southward longshore current carried each float along the beach. He reported average velocities of the floats to be about 0.5 knots (25 cm per sec).

Tollefson also conducted fixed-float observations during the summer months of 1958. Each float had an attached buoyant tag line which could be monitored from an elevated beach position. The direction of the tag line relative to the fixed float indicated the direction of the current. The area surveyed was less than a square mile, and again apparently included the waters inside the surf zone. Tollefson observed that the currents often exhibited an eddy-type pattern which he thought to be a function of the stage and height of the tide and the depth of the water. These currents could be intensified by the prevailing wind direction. The frequency of eddy currents was inversely proportional to the depth of water with very few occurring in water deeper than seven meters. Grouping the wind directions into either north or south, he found that the current directions, when similarly grouped, were nearly 100% in agreement with the wind. Tollefson did not mention the longshore current regime which is quite distinct from the currents beyond the breaker zone.

On the basis of Tollefson's study, a new outfall was planned and constructed in 1965, 1.5 km offshore. The new outfall consists of a y-shaped diffuser in ten meters of water.

Breaker heights, periods and angles of wave approach were reported by Hall (1962) for observations taken every four hours by personnel of the Yaquina Bay Lifeboat Station during the period of 1955 to 1959. About 50% of the observed breaker heights were greater

than two meters, and about 10% were higher than five meters.

Gonor et al. (1970) recorded daily sea-surface temperature and salinity during 1968 and 1969 at the northeast corner of the bight. These water samples, taken from the beach, apparently exhibited the influence of several nearby streams since salinity values were very low during periods of high runoff. The trend of the temperatures indicated gradual cooling from September 1968 to January 1969, and continuous warming from January to June 1969. An interruption of the warming trend occurred in late June with the advent of upwelling. Salinity values similarly decreased and increased at the same time as the temperature did except during periods of upwelling, when higher salinity values were found.

No further studies have been reported in this area.

METHODS AND PROCEDURES

Sea Water Samples

The temperature of the pulp mill effluent is about 30°C as it flows through the conduit pipe under the beach. Furthermore, it contains essentially no dissolved oxygen and a very low salinity value. The large rate of discharge (about 38 million liters per day) (CH_2M Eng. Rpt., 1965) could be expected to influence the waters within the bight. Sea water temperature, salinity (hence density), and dissolved oxygen content are important parameters of ocean outfall sites because they may be used as indicators of water types and water movements. Pattullo and Denner (1965) used density as an aid in determining the origin of water samples taken along the Oregon coast. (Density is not measured directly but is computed from the temperature and salinity of the water sample.) Temperature is often used to characterize a water type because of the relative ease of measurement and because temperature is considered to be a conservative property of water.

A thermistor probe was constructed to give temperature accuracy of about $\pm$ 0.05°C. In addition, a mechanical bathythermograph (BT) was used during the latter half of the study to give a continuous trace of temperature versus depth. The BT trace showed any tendency of stratification which might otherwise be missed using only the thermistor probe. The BT, calibrated against the thermistor

probe and high-quality laboratory thermometers, was considered accurate to at least $\pm$ 0.2°C.

Salinity and dissolved oxygen values were obtained from water samples taken with a Frautchi bottle and analyzed by personnel at the Oregon State University Marine Science Center. The dissolved oxygen samples were treated with reagents immediately after they were taken and then preserved. They were analyzed several hours later by a modified Winkler method. Salinity samples were analyzed with a laboratory inductive salinometer.

Water samples were taken at several locations upstream and downstream from the outfall. Exact locations were not chosen because of the difficulty of maintaining a specific position. The boat experienced considerable drift in a wind and its navigational equipment was not suitable for the accurate positioning required. All water sampling was done from Oregon State University's R/V Paiute, a ten meter boat used primarily for calmer conditions and inside the estuary. When large waves and swell or fog were present, the Paiute could not be taken into the bight. On many occasions the sea conditions were marginal so that only one rapid sample could be taken before leaving the area.

Four locations were sampled when weather conditions were favorable. The first and most important station was directly over the outfall. The next station was in the effluent plume about 150 meters

downstream from the outfall. A third station was upstream from the outfall plume. The fourth station was located seaward of Yaquina Reef (about 1.6 km west of the outfall). The latter two stations represented uncontaminated water. Preliminary studies involved taking many samples from numerous stations inside the bight. However, it was soon determined that all the water in the bight was usually nearly homogeneous and that differences which were found were related to the outfall effects.

Nearshore Currents

Currents play an extremely important role in distributing an effluent. However, reliable current measurements in the nearshore environment are difficult to obtain.

The methods of measuring currents are typically classified as either Eulerian methods or Lagrangian methods. The former applies to measurements at a fixed point such as a platform or an anchored buoy by a current meter which senses both speed and direction of the water mass as it passes by. The latter method traces the path of a water particle throughout a period of time. Examples of this type include "tagging" the water particle with dye, radioactive material, or neutrally buoyant objects. Both the Eulerian and Lagrangian methods have unique advantages and disadvantages depending on the requirements of the user, the expense involved, the area of study,

and other factors.

The current meter may produce a continuous record of the currents at a fixed position. Relating currents to winds, tides, and waves requires a knowledge of the response of the current to these current-producing forces; however, current meters are quite expensive and difficult to maintain in the nearshore zone. Synoptic studies, involving several current meters recording simultaneously, increase the cost proportionately. Furthermore, data processing can become expensive, and data analysis can be in error if unknown high-frequency variations alias the data (Webster, 1964). Yaquina Bight is a high-energy zone (heavy surf and large waves frequently occur), where current meters and mooring systems may be easily damaged.

Lagrangian methods also present problems. The time required to follow a "slug" of tagged water may be excessively long, and the errors of positioning may be greater than the advection of the water. Adverse weather conditions can be as detrimental to the Lagrangian methods as to the anchored meters, particularly in the shallow coastal waters where breaking waves are a hazard to a small craft used for placing the tag or observing the marker. However, the Lagrangian method does have the advantage of measuring the net flow over the period of observation with no aliasing. Consecutive observations of a marker can provide a trajectory. The use of aircraft to observe and deliver the tagging material allows work in nearly all

types of weather in the nearshore zone. The observational time interval can be varied according to flow rates observed.

For current studies off South Africa, Welch (1967) used a dye package dropped from an aircraft which provided an anchored reference marker and a drifting drogue. Both the reference marker and the drifting drogue continuously released dye which allowed rapid identification from the air. The current speed was determined by measuring the distance the drifting drogue had traveled from the reference marker during a known period of time. This method was chosen as the most feasible for the Yaquina Bight study.

Many modifications of Welch's dye package were required before it functioned properly in Yaquina Bight. The powdered dye was replaced with a solid toroid dye cake, and the method of releasing the tether line from the anchor was changed. A description of the dye package used in the bight follows. A standard juice can (17.5 cm high and 10 cm in diameter) was weighted with approximately 1 kg of lead or with steel shot covered with melted paraffin. The can containing the floats sank after hitting the water and tethered the reference marker. Nylon line (19 meters) was wound on a discarded film spool and mounted inside the juice can; a metal shaft was used as an axle. One end was attached to the spool and the other end to a round styrofoam float. A toroid cake of fluorescein dye was attached to the float. A second float with an attached cake of rhodamine-B dye

was connected by two meters of line to a 30 x 9 cm cloth drogue. The drogue would then deploy at a depth of two meters while the surface float was discharging dye, producing an easily-recognized marker. The two floats were enclosed in a water-soluble plastic bag. Upon entering the water, the plastic would dissolve and the drogue would move away from the anchored float. A diagram of the package is shown in Figure 2.

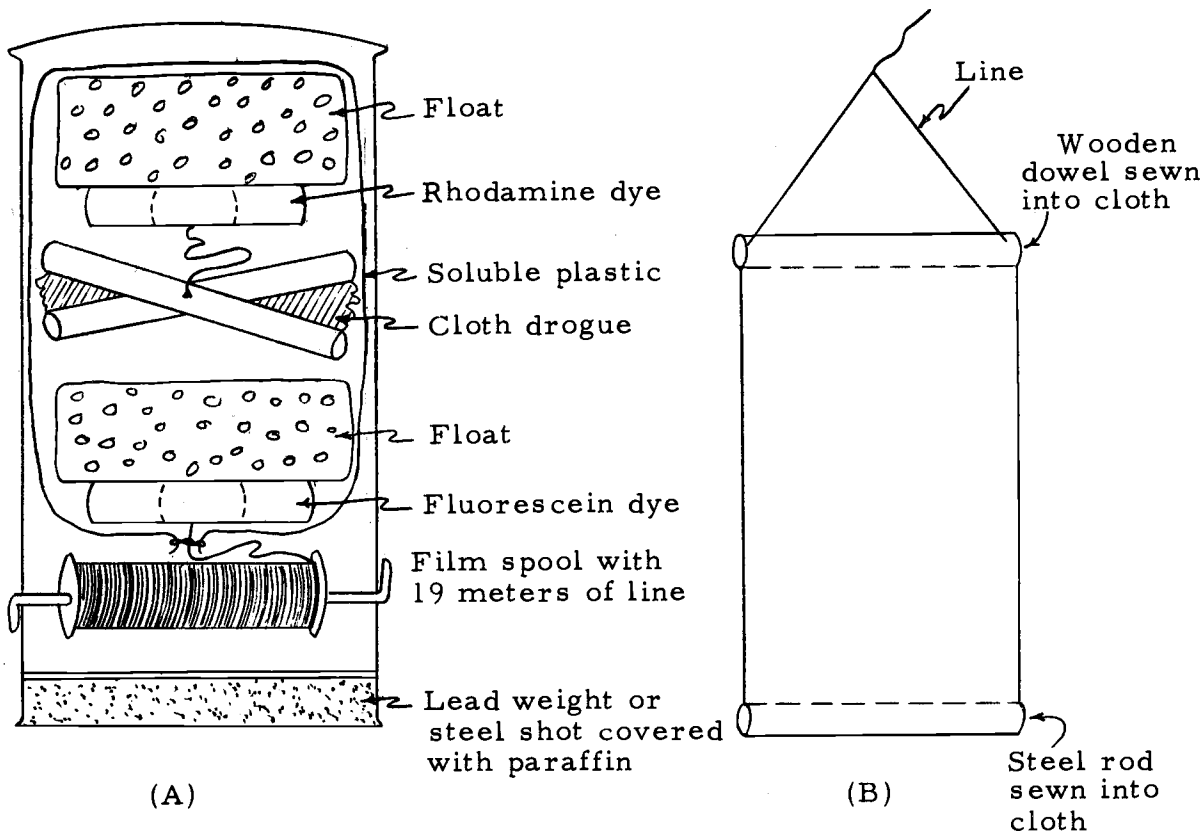

Figure 2. Diagram of the modified dye package (A), and the cloth drogue (B).

The dye package was dropped from an airplane flying between 60 and 150 meters at several selected locations within the bight. The time of the drop was recorded. The water soluble plastic film dissolved within 20 seconds, and the drogue and its float drifted off with the current, while the tethered float remained, releasing a trail of green dye. After the drogue had drifted for some distance, its displacement from the tethered reference was measured by two methods. One method was visually sighting on both floats with the tips of a pair of dividers held a fixed distance from the eye. The angle between the two floats was noted, and by triangulation the speed was calculated by the formula

$$V = \frac{2\,H \tan(1/2\,\theta) + (19^2 - h^2)^{1/2}}{dt}$$

where H is the aircraft altitude at time of measurement, h is the water depth, θ is the angle subtended at the plane (see Figure 3), and dt is the elapsed time between the drop and observation. The term $(19^2 - h^2)^{1/2}$ is the distance in meters traveled by the reference marker before the tether becomes taut.

The second method was taking color photographs of the floats with a 35 mm camera. The door of the aircraft was removed before each flight to allow the observer to take vertical pictures. At an altitude of 460 meters the 5.0 cm styrofoam floats were easily seen. The time of the photograph, the altitude, and the direction of flow

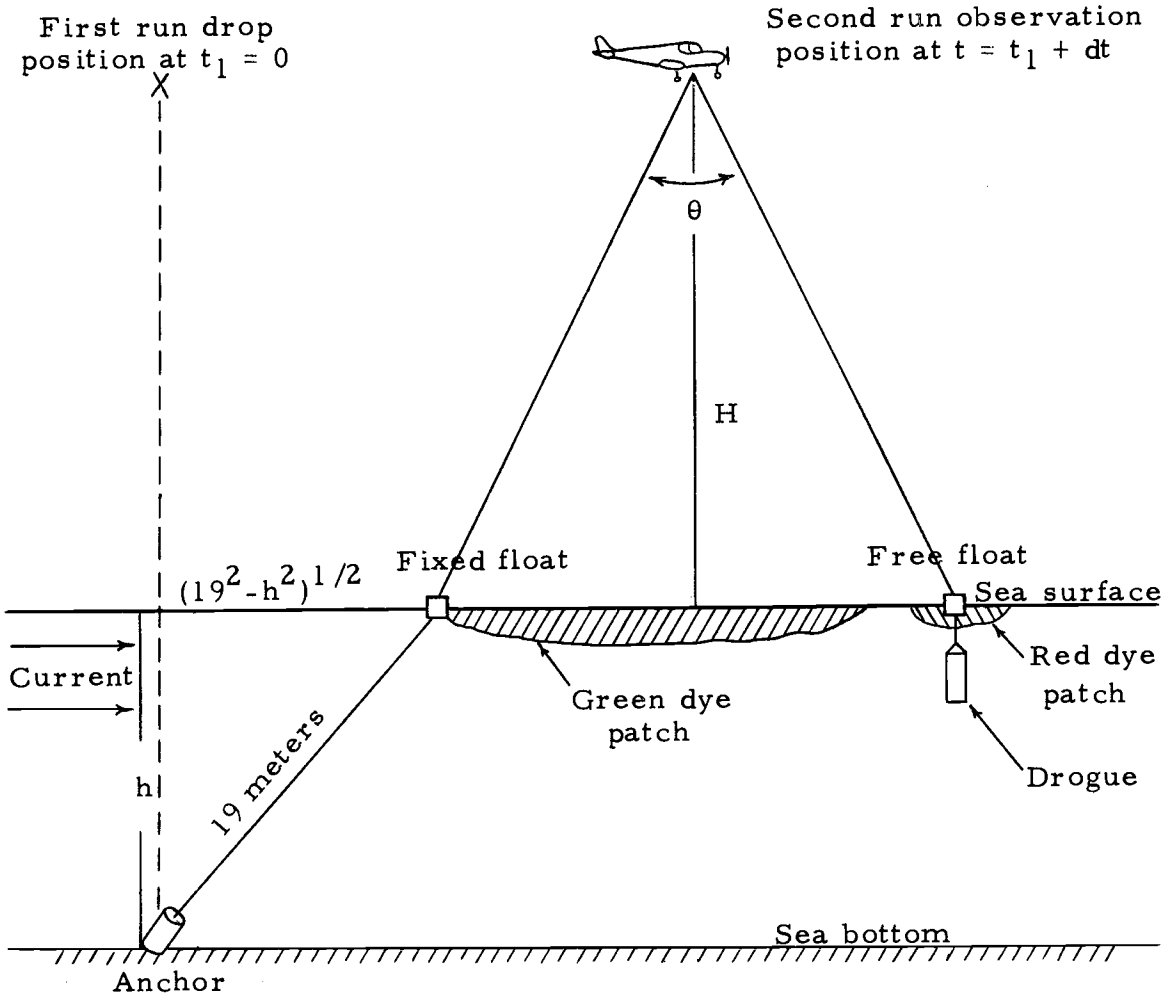

Figure 3. A schematic diagram of the dye-package after deployment.

(determined from the plane's heading) were noted during the observations. After the film was developed and the photographic slide was projected on a screen, the distance between the floats was obtained by the following equations:

$$\text{(a)}\quad L = \frac{35H}{f} \qquad\qquad \text{(b)}\quad X = \frac{LB}{C}$$

where L is the width of the field of view on the water surface, H is the altitude, f is the focal length of the camera (in mm), 35 is the width of the film in mm, X is the actual separation of the floats on the water, B is the distance between floats (as measured on the screen), and C is the total width of the slide as projected on the screen.

The photographic method proved to be quite accurate. Tests taken over the airport runway at Newport, Oregon indicated the 47 meter-wide runway to be 47.2 meters wide, an error of less than 0.5%. Although the visual method may appear redundant, it often gave a displacement value when the photographs were not properly exposed or if other conditions prevented an accurate measurement on the film. Remarkably close agreement was noticed between the two methods when both were obtained for the same dye marker.

Four locations within the bight were selected for the aerial current measurements. These are indicated in Figure 1 by an X. The outfall location was directly over the effluent outfall. The second location was west of Big Creek, about 1.6 km south of Yaquina Head.

The third and fourth stations were several hundred meters from Yaquina Head and the north jetty, respectively.

Current measurements were made in nearly all types of weather, including heavy rains, snow, freezing temperatures, and winds greater than 20 knots. High winds made it difficult to locate the markers in the water since the surface was frothy. Furthermore, the increased turbulence in the water tore the markers up and dispersed the dye too rapidly. Handling of the aircraft in the accompanying turbulence also made observations more difficult.

Each aerial current observation was accompanied by nearly simultaneous beach observations of the wind, tide, and waves. These three variables were convenient to measure and were assumed to be the major components of the observed currents in the bight. This is not to say that other factors were not important, but that other factors such as the mean oceanic current, inertial currents, hydraulic currents and eddies were not susceptible to measurement and analysis by this technique.

To relate the current producing forces, i.e., wind, tide, and waves, to the observed current, each measurement was separated into north-south and east-west vector components. The wind, wave, and tide components were treated as independent variables in the regression analysis, while the observed current was the dependent variable. However, the regression analysis requires the dependent

variable to be a linear function of the independent variables. A number of the accepted methods to linearize current producing forces are examined in this study to determine which ones can best predict the currents measured in the bight. The linearization of each variable is discussed separately later in the text.

Winds

Wind velocity was the most important current producing variable measured. Ideally, the anemometer should be located in the same area as the current measurements. When the project was initiated, the Pacific Northwest Water Resources Laboratory maintained a continuously recording anemometer installed on the south jetty of Yaquina Bay. This instrument was very convenient and accurate. Unfortunately, its operation was discontinued in January 1969. We then used a hand-held anemometer. A hand-held anemometer is not entirely satisfactory because a five-minute observation period is too short to determine the hour's average wind. Wind velocities prior to the measurement time were also needed but it was not practicable to do so by this method. Although topographic features of the coastline affect the wind speed and direction and are difficult to compensate for, wind measurements were necessarily taken from the beach. The hand-held anemometer was used only temporarily until a continuously recording anemometer was installed. It was

installed in March 1969 near the south jetty. This anemometer recorded wind speed in miles per hour and the wind direction as a fraction of the hour the sensor was within 65^{o} of a cardinal point. For example, an hour's direction was given as a fraction of the time in the north direction, a fraction in the west direction, etc. By considering the fractions as unit vectors, the mean direction could be resolved. However, due to the recording mechanism, accuracy of the instrument was not constant but rather depended on the variability of the wind direction. As the winds became less variable, the accuracy decreased statistically. Under conditions of a steady wind direction, accuracies decreased to $22\text{-}1/2^{o}$ which is not accurate enough when relating direction of the currents to wind direction. In view of several alternatives, however, it served as the best source of wind data available.

Much theoretical and empirical work has been done on the relationships of the independent current producing variables and the observed current. The wind induced current has received particular attention since 1905 when Ekman first derived the theory of pure drift currents in the deep ocean. More recently, Welander (1957) generalized Ekman's theory to apply in shallow water where the depth of frictional influence is given by the depth of the water. However, several assumed conditions of the theoretical treatment which do not lend themselves to this study are: the ocean is in a steady,

unaccelerated state; the eddy viscosity coefficient is constant with depth; and tidal, hydraulic, or other currents are absent.

In empirical studies attempts have been made to relate the current velocity to the wind velocity or to the wind stress. Wind stress, τ, is conventionally determined as $\tau = \rho' C W^2$, where ρ' is the density of the air, W is the wind speed, and C is a dimensionless "drag" coefficient. The value of C is a contested subject, as shown by Roll (1965). Many workers have considered C as either a constant or as a variable that increases with wind speed. It also has been shown to vary with anemometer height above the water surface. Wu (1969) analyzed 42 experimental investigations, 12 laboratory studies, and 30 oceanic observations to determine the drag coefficient for oceanic applications under various wind conditions. He concluded that the coefficient could be approximated by $C = 1.25 \times 10^{-3} / (W_{10})^{1/5}$, for wind velocities less than one meter per second, where W_{10} indicates the winds measured at an anemometer height of ten meters. For wind velocities between one and 15 meters per second, $C = (0.5)(W_{10})^{1/2} \times 10^{-3}$, and for winds greater than 15 meters per second, $C = 2.6 \times 10^{-3}$. (The latter value was Ekman's (1905) estimate of C for all wind speeds.)

Using Wu's approximations for the drag coefficient, a wind stress term was then calculated by the expression $\tau = CW^2$. The density of the air was not included because it was not determined for

each observation but was assumed to be relatively constant. Therefore, it would have had little affect on the stress term in the regression analysis.

To determine which wind component appeared most closely related to the observed current, a wind velocity term was tried as well as a wind stress term. Both terms were calculated for the average winds during the three time periods; (1) the hour of current observation, (2) the hour previous to the observation, and (3) two hours prior to the observation.

Additional terms in the regression analysis were obtained by averaging the present and past winds. A weighted scheme was also attempted, whereby the wind-stress term of the present hour was weighted by a factor of three, the previous hour's term by two, and the wind of two hours previous by one. After each of these terms had been calculated, the vector components acting in the north-south and east-west planes were obtained by $(Wi \cos(\theta - 180^{\circ}))$ and $(Wj \sin(\theta - 180^{\circ}))$, where Wi and Wj are the wind terms in the north-south and east-west planes respectively, and θ is the wind direction. The subtraction of 180° simply changed the direction of wind approach to direction of wind flow to be compatible with the current flow direction.

Wave Measurements

Waves are of practical importance in the matter of outfall

construction, and the turbulence caused by waves and breakers increases the diffusion of the effluent. Waves also induce currents which affect the dispersion of effluents. Kinsman (1965) states that currents induced by waves may reach 1% of the wave speed. Therefore, a significant contribution to water motion in the bight would be expected from the large waves and breakers which occur along the Oregon coast, particularly during winter months. The wave induced current has been considered in this study.

Most wave studies of a general nature consist of observing the breaker height, period and angle of approach. Deep water and shallow water wave heights can then be obtained from a combination of Airy wave and solitary wave theory. The wave period is assumed to remain constant when a deep-water wave shoals (i.e., the wave height increases and both wave length and celerity decrease).

Breaker heights and periods were recorded on the beach during the longshore current measurements. The wave period was determined by recording the time interval during the passage of 11 wave crests (ten complete waves), and dividing by ten. This was repeated five or six times during each observation, and the results averaged to give the wave period.

The breaker heights were measured by lining up the breaker crests with the horizon as the observer stood at the prevailing sea level. The height of the observer's eye was determined by inserting a

2.3 meter pole, marked off in 0.3 meter sections, 0.3 meters into the sand at a point (representing still water level) midway between the uprush and backwash of the waves. The observer stood farther up the beach and lined up the horizon and the breaker crests and recorded the height on the pole. If the breakers were higher than the pole, the observer inserted a second similar pole further back from the water (Figure 4). The observer then lined up the horizon and the wave crests on the second pole and recorded the height of the first pole (2.0 meters) plus the distance between the horizon-first pole top intersection and the horizon-breaker height intersection (Δy).

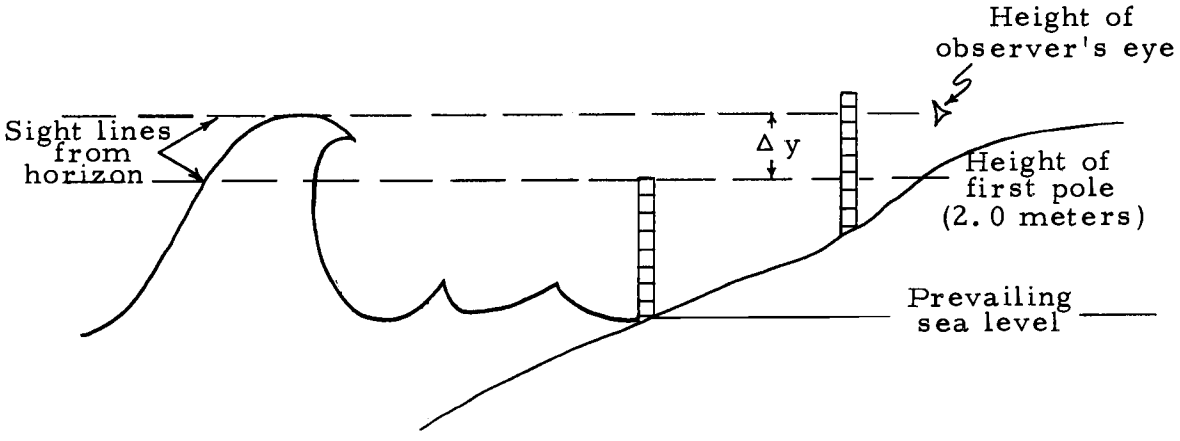

Figure 4. Illustration of the breaker height determination method.

The breaker height required is the height of the breaker crest above the trough. The wave trough is depressed below the still-water level, so the observed breaker height is multiplied by four-thirds to give the true height of the breakers.

The direction of wave approach is very difficult to measure accurately, particularly from shore since the waves refract as they reach shallow water and approach the beach at very small angles. To improve direction measurements, the deep water wave approach was observed from the airplane. The pilot would adjust the course of the airplane until it was perpendicular to the wave crests and the observer would record the plane's heading as the direction of wave approach. On several occasions, significant waves could be distinguished approaching from two directions; both directions were then recorded.

The wave component of the observed current is generally quite small. First order wave theory requires water particles to move in closed orbits, but Stokes (1880) derived a theory of irrotational waves which provides for a slow drift in the direction of wave propagation. In deep water, a wave induced current, U, is calculated by the equation $U = a^2(2\pi/L)^{3/2} g^{1/2} e^{-4\pi z/L}$, where a is wave amplitude, L is wave length, g is gravitational acceleration, and z is the depth beneath the surface at which the current is calculated.

Longuet-Higgins (1953) investigated the effect of viscosity as a wave propagates through water of finite depth. When the ratio of the wave amplitude to the boundary layer thickness is small (on the order of 0.5 mm) he found wave drift currents could be determined by his conduction solution,

$$U = (a^2\pi^2/TL \sinh^2 kd)\,[(2 \cosh 2kd(z/d-1)) + 3 + kd \sinh$$

$$2kd(3z/d - 4z/d+1) + 3\,((\sinh 2kd/2kd) + 3/2)(z^2/d^2 - 1)]$$

where d is the still water depth, T is the wave period, and k is the wave number ($2\pi/L$).

When the wave amplitude is large compared with the boundary layer thickness, as it was in this study, the conduction solution does not apply, as vorticity is transported along streamlines by convection. Neither Stokes' nor Longuet-Higgins' solution is theoretically applicable. Stokes' solution does not consider an inviscid fluid nor bottom friction, while Longuet-Higgins' solution provides only for extremely small waves. However, both solutions have given values comparable to observed drifts and are thus useful in a prediction equation.

Russel and Osorio (1958) examined drift profiles in a closed channel and found that when the value of $2\pi d/L$ ranged from 0.7 to 1.5, Longuet-Higgins' conduction solution predicted these drift velocities well. Russel and Osorio found that Stokes' equation predicted the drift in deep water (when $2\pi d/L$ exceeded 1.5).

To determine which equation provided the better prediction, one term to be used in the regression analysis for the wave-induced current was obtained from the Stokes equation and a second term from Longuet-Higgins' equation. A third term was derived from a selection between the first two based on the value of $2\pi d/L$;

Longuet-Higgins' value was used when the particular wave parameter of $2\pi d/L$ was between 0.7 and 1.5. Otherwise, the value from Stokes' solution was used. Each of the three terms was then transformed into north-south and east-west components to become the wave-induced current variable.

Tide Measurements

The periodic rise and fall of the sea level in response to the passage of the moon and sun give rise to the reversing tidal currents characteristic of estuaries and narrow channels along a seacoast. In the open ocean, tidal currents are usually rotary, due to the rotation of the earth relative to the sun and moon. Over shallow bodies of water the tidal currents are dependent on the character of the tide, the water depth, and the coastal topography (Leipper, 1955). The tidal currents at any specific location are as regular as the tide which produces them. Very accurate estimates of the tidal currents over the continental shelf can be obtained by power spectrum analysis of moored current meter records (Collins, 1968). Attempts were made during calmer summer conditions to measure tidal currents using mechanical current meters, but instrument malfunctions prevented an analysis of the tidal motions by this method.

The tidal currents can be inferred for an area if the range and duration of the tide are known. The closest tide gauge was located at

the Marine Science Center near Yaquina Bay. Since the gauge is located within the Yaquina estuary it does not record the tides exactly as they occur in the bight, but the relative range of the tidal height and duration can be considered essentially the same.

Fleming (1938) derived an equation for tidal current velocity as a function of the amplitude of the tide, the distance from shore, and the depth of the water. The velocity, U, is given by

$$U = (\sigma / d) \sin (\sigma t) \int_0^x A \, dx$$

where $\sigma = 2\pi / T$, T is the period of the tide, d is depth of water, t is time (always less than or equal to T), A is the amplitude of the tide, and x is the distance from shore.

If we assume that the amplitude is constant from the beach to the outfall (a distance of about 1400 meters), the maximum tidal current velocity (when $\sin \sigma t = 1$) is $(\sigma / d)Ax$. For a tidal amplitude of 1.2 meters, a distance offshore of 1400 meters, a water depth of ten meters, and a period of 12-1/2 hours, the maximum theoretical current is about 2.5 cm per second.

The data for this study consisted of the duration of the tidal stage, the range of the tide, and the fraction of the tidal period elapsed at the time of observation. The tide was assumed to be a standing wave so that the maximum current would occur midway between high and low tide. Furthermore, it was assumed that the maximum currents occurred in the north-south plane with currents of

lesser magnitude occurring in the east-west directions. Near the beach the tidal currents are assumed to run nearly parallel to the shore; the bottom topography appears to enhance this assumption (i. e., the Yaquina Reef runs nearly parallel to a north-south line).

The tidal term for the regression analysis was determined by calculating the fraction of the maximum current based on Fleming's equation. Periods of slack tide produced a computed tidal current of zero while mid-tide calculations produced the maximum value of the tidal current. The component obtained in this manner was used for both the north-south and the east-west regression term.

Longshore Currents

The movement of water parallel to the coast inside the breaker zone is called the littoral or longshore current. This current is thought to be caused by waves breaking obliquely to the shore with the current velocity being proportional either to the incoming wave energy or momentum of the water particles. It has been shown experimentally in the laboratory (Galvin and Eagleson, 1965) and theoretically by Longuet-Higgins (1970) that the current velocity varies with distance from the shore. Maximum velocities are found near the middle of the surf zone (i. e., halfway between the breakers and the beach).

Measurement of the longshore current has presented many

problems to researchers. Current meters are not used because of the turbulence in this zone and the abuse the meters receive from the breaking waves, especially when the breakers are large. A commonly used method is to inject a fluorescent dye into the surf and measure its movement with a fluorometer. Although this is ideal for beaches with little wave energy, heavy surf precludes observers working in the area or being able to distinguish advection of the dye from diffusion. The Oregon coast usually has heavy surf and therefore dyes were not used.

Plastic bottles (100 ml capacity) painted bright orange and filled with water to achieve a very slight positive buoyancy were dropped into the surf zone from the aircraft and their drift rate was used as a measure of the longshore currents. The pilot would fly seaward perpendicular to the shoreline and as the plane passed over the beach at low altitude, the observer would drop four numbered bottles, one at a time, into the surf zone. At slow speed the bottles could be dropped quite accurately at the desired locations. The drop time was noted by both the airborne observer and the observer on the beach who, in most instances, was directly under the plane as it passed overhead. As the bottles washed ashore the beach observer would mark the time of grounding and pace off the distance to the bottle. Velocity of the current was obtained by the relationship $V = S/t$, where S is the distance traveled parallel to the beach and

t is the elapsed time. This method appeared to be expedient and inexpensive since the plane was in the same general area for other measurements. From observations during the course of the study, bottles which were dropped beyond the breaker zone did not wash ashore for some time, if at all, so that the bottles which were recovered probably gave a mean current throughout the surf zone. An interesting observation which occurred many times was that the bottles dropped into the center of the surf zone very often not only traveled the farthest but also reached shore before those dropped closer to the beach, indicating a greater current velocity midway in the surf zone.

RESULTS AND DISCUSSION

Hydrographic Data

Values of temperature, salinity, dissolved oxygen content, and σ_t (density) at the outfall station were plotted versus time for the observation period from October 1968 to August 1969. Because the outfall area was of primary concern, the other three stations are referenced to the outfall station. The upper traces (a) in Figures 5, 6, 7 and 8 are plots of the outfall surface and bottom temperature, salinity, oxygen and σ t, respectively. The lower traces in each figure are plots of the deviations from the outfall station values of the data at the stations (b) in the effluent plume, (c) out of and upstream from the effluent plume, and (d) seaward of Yaquina Reef. This presentation allows rapid comparison of the other stations to the outfall station. It should be noted that about half the observations occurred during June, July and August when the weather allowed more work days. Some bias may therefore be present; nevertheless, the deviations at each station are fairly consistent throughout the year.

Table 1 lists the mean values of temperature, salinity, σ t, and dissolved oxygen content for the water at the four stations over the period of observation. The entire year was divided into four "seasons," based on similarities of the data. The seasons are (1) September through November 1968, (2) December 1968 through March

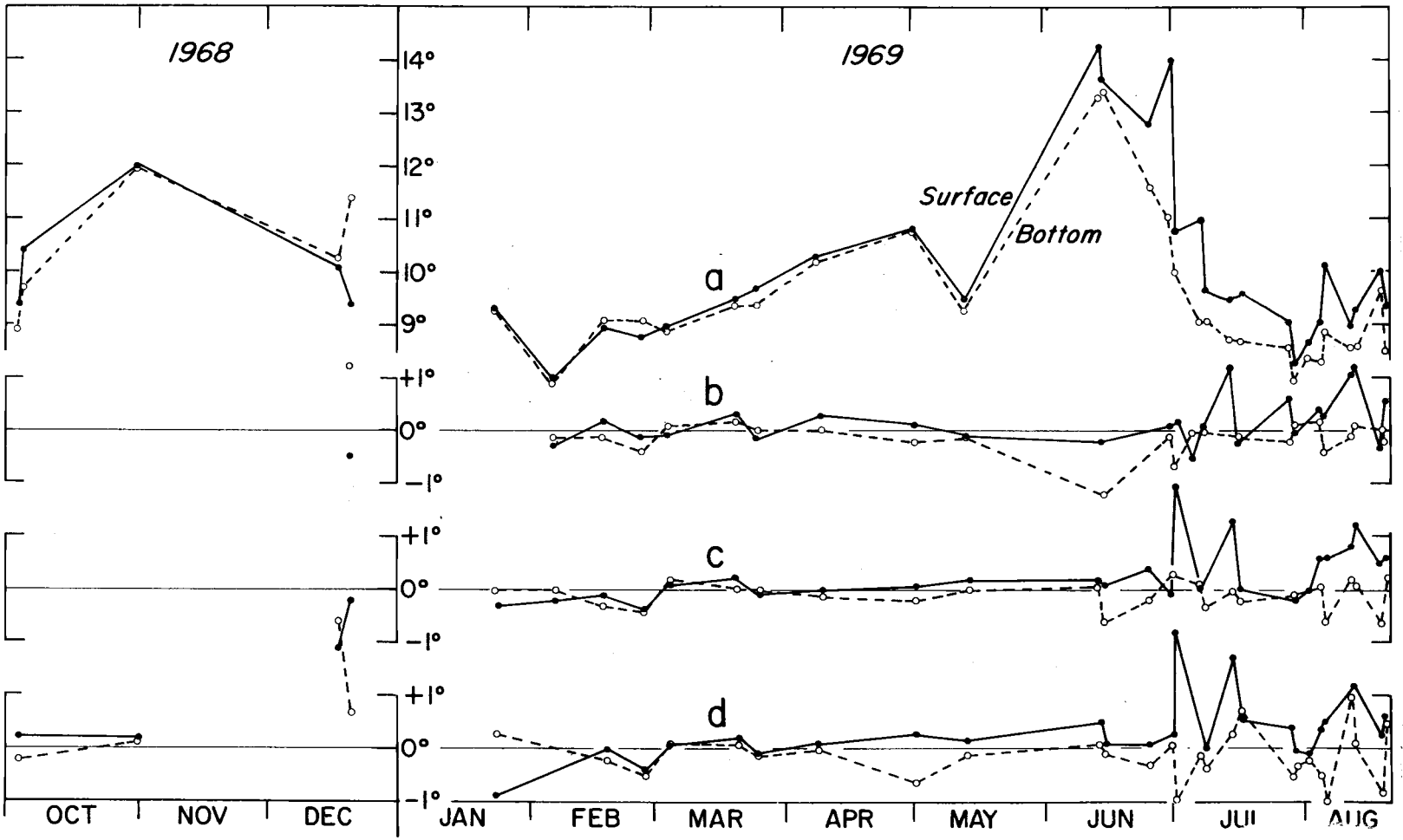

Figure 5. Water temperatures from October 1968 through August 1969. The upper traces (a) snow surface and bottom temperatures at the sewer outfall. The lower traces show the deviations from temperatures at the outfall:(b) in the plume (c) out of the plume and (d) outside the reef.

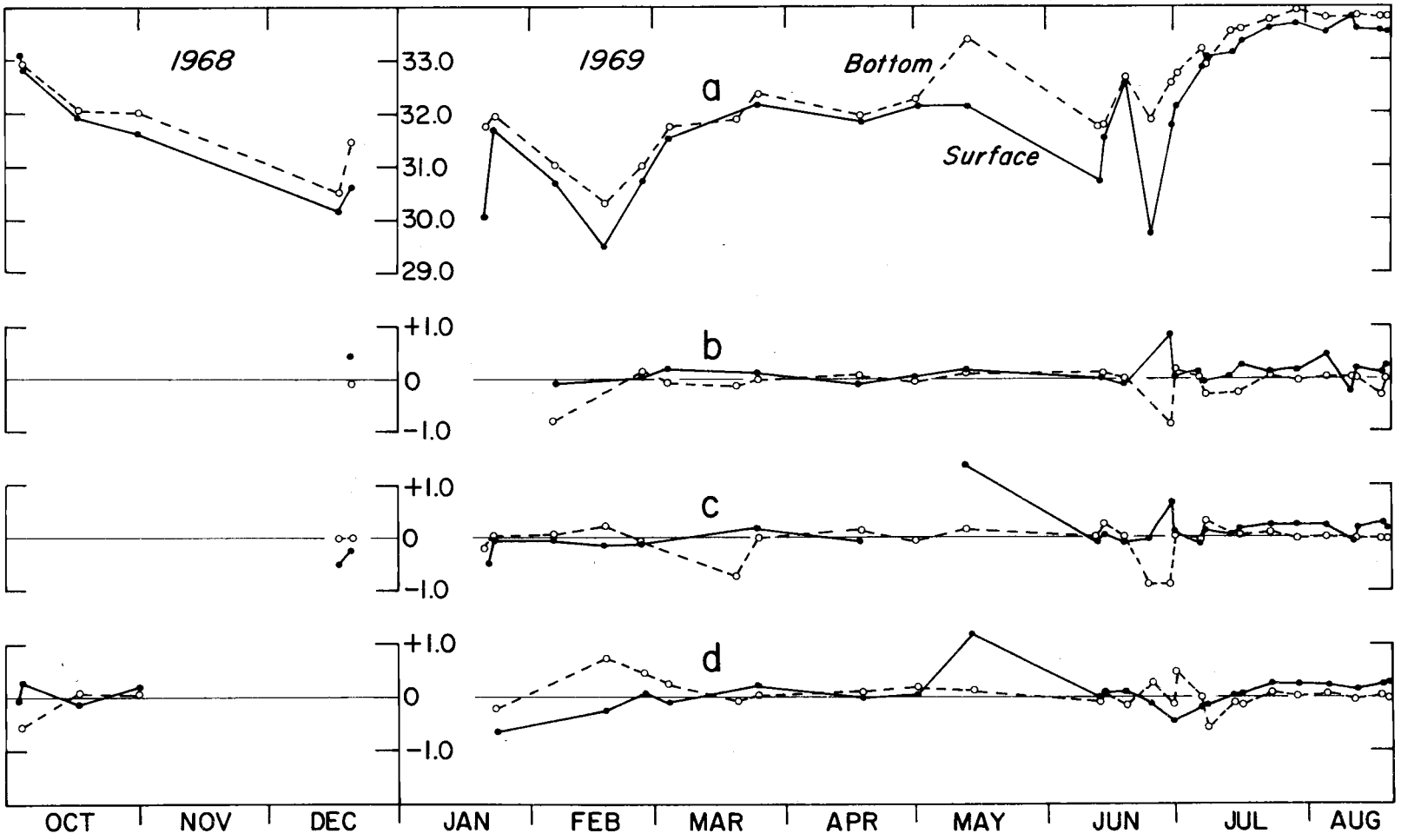

Figure 6. Salinity at the outfall during the period October 1968-August 1969. The three lower lines show deviations from outfall salinities (b) in the plume (c) outside the plume and (d) outside the reef.

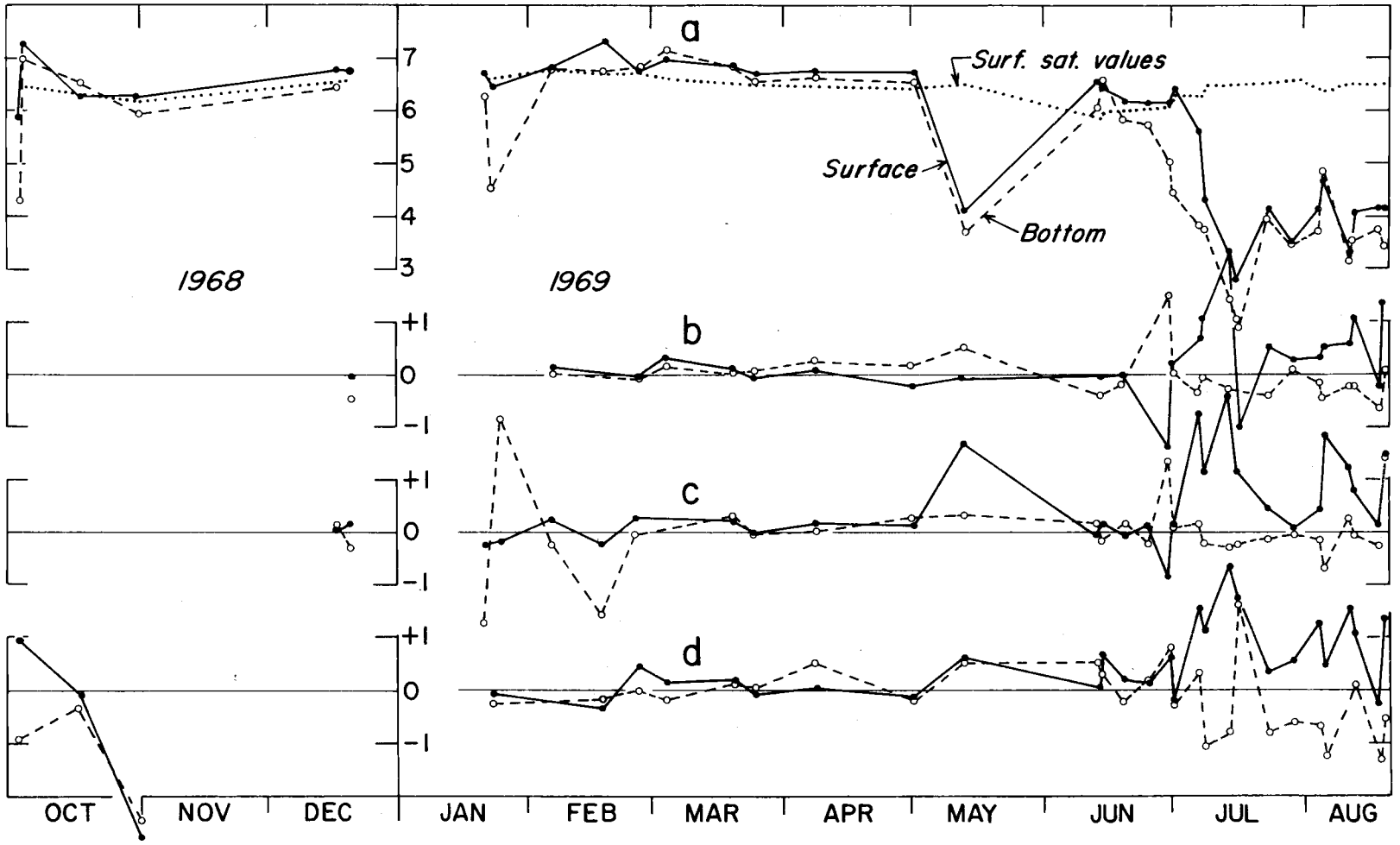

Figure 17. Dissolved oxygen concentrations at the outfall in ml/liter (October 1968-August 1969). The dashed line in the upper plot indicates saturation values. The lower traces are deviations from outfall concentrations (b) inside the plume, (c) outside the plume and (d) outside the reef.

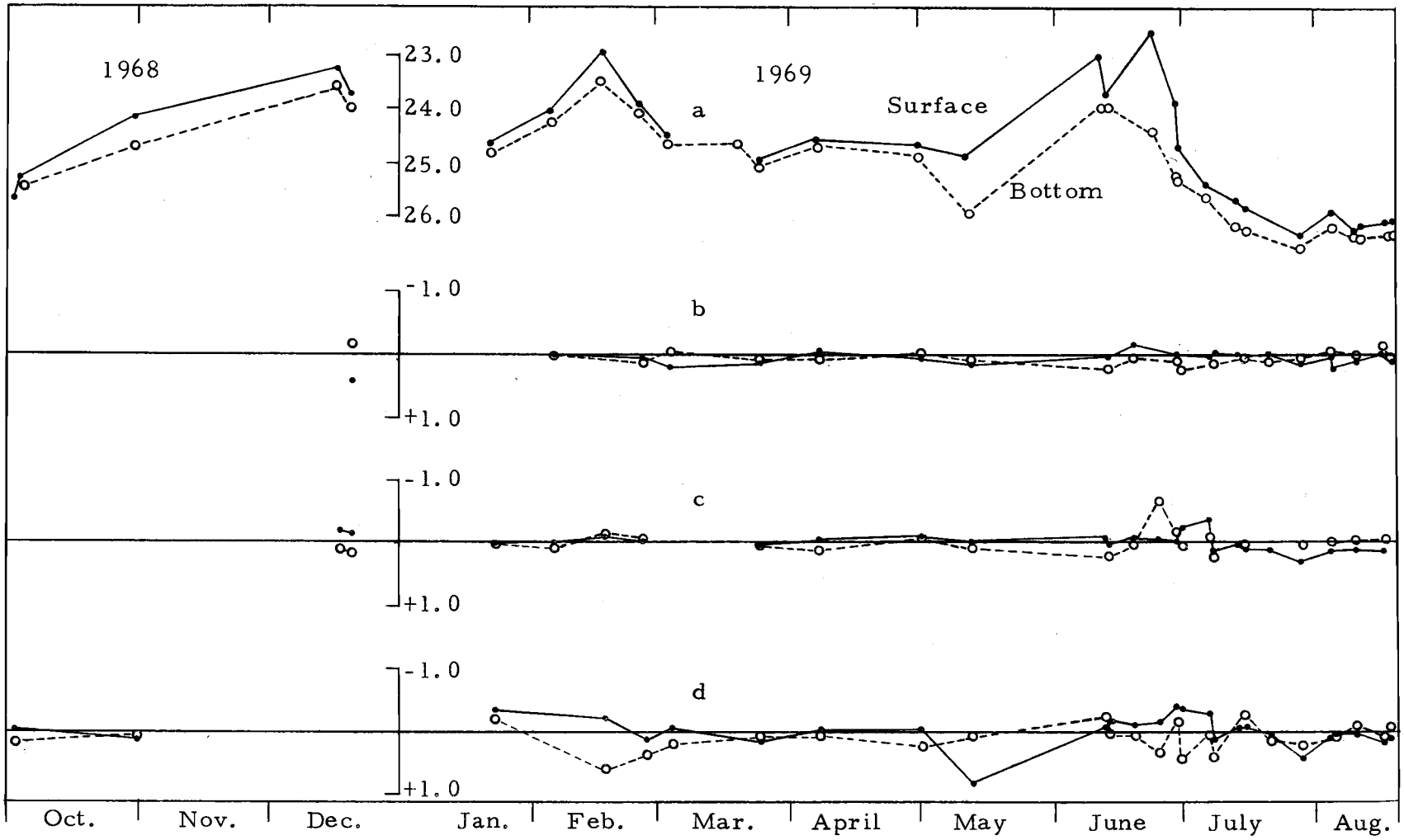

Figure 8. Sigma-t at the outfall during the period October 1968-August 1969. The three lower lines show deviations from the outfall σ-t (b) in the plume, (c) outside the plume, and (d) outside the reef.

Table 1. Temperature, salinity, σ-t and dissolved oxygen content in Yaquina Bight during the period of observation.

Season	Parameter	Outfall		In plume		Out of plume		Outside reef	
		Mean	Standard deviation	Mean	Standard deviation	Mean	Standard deviation	Mean	Standard deviation
Sept./ Nov.	Temperature	10.26	(1.16)	-	-	-	-	10.59	(1.17)
		9.79	(1.44)	-	-	-	-	10.26	(1.86)
	Salinity	32.530	(.676)	-	-	-	-	31.926	(1.400)
		32.622	(.591)	-	-	-	-	32.632	(.786)
	σ-t	25.12	(.72)	-	-	-	-	24.50	(1.37)
		25.38	(.72)	-	-	-	-	25.14	(.99)
	O_2	6.09	(.88)	-	-	-	-	5.94	(1.40)
		5.61	(1.26)	-	-	-	-	4.51	(1.43)
Dec./ March	Temperature	9.05	(.56)	8.76	(.72)	8.78	(.64)	8.87	(.54)
		9.17	(1.01)	9.00	(1.01)	8.89	(.54)	8.94	(.37)
	Salinity	30.873	(.829)	31.328	(.632)	30.624	(.995)	31.022	(1.024)
		31.409	(.661)	31.575	(.487)	31.083	(.751)	31.754	(.467)
	σ-t	23.93	(.69)	24.30	(.42)	23.76	(.74)	24.05	(.78)
		24.29	(.54)	24.46	(.36)	24.22	(.53)	24.61	(.34)
	O_2	6.80	(.23)	6.86	(.24)	6.80	(.28)	6.84	(.29)
April/ June	Temperature	12.04	(1.95)	11.55	(1.83)	12.05	(1.87)	12.06	(1.91)
		11.13	(1.48)	10.54	(1.01)	11.16	(1.46)	11.02	(1.58)
	Salinity	31.548	(.916)	31.990	(.370)	31.790	(1.45)	31.664	(1.069)
		32.283	(.579)	32.501	(.619)	32.218	(.74)	32.339	(.545)
	σ-t	23.91	(.95)	24.34	(.55)	23.94	(1.21)	23.99	(1.12)
		24.66	(.68)	24.93	(.62)	24.60	(.76)	24.72	(.67)
	O_2	6.12	(.86)	5.78	(1.10)	6.17	(.52)	6.44	(.76)
		5.77	(.98)	6.02	(.99)	5.88	(.86)	6.24	(.90)

(Continued on next page)

Table 1. (Continued)

Season	Parameter	Outfall		In plume		Out of plume		Outside reef	
		Mean	Standard deviation	Mean	Standard deviation	Mean	Standard deviation	Mean	Standard deviation
July/ Aug.	Temperature	9.49	(.59)	9.93	(.53)	9.98	(.98)	10.20	(1.12)
		8.82	(.52)	8.73	(.35)	8.69	(.37)	8.65	(.63)
	Salinity	33.296	(.439)	33.420	(.489)	33.469	(.519)	33.535	(.399)
		33.593	(.369)	33.626	(.307)	33.632	(.341)	33.639	(.286)
	σ -t	25.70	(.41)	25.75	(.43)	25.75	(.54)	25.71	(.60)
		26.07	(.33)	26.11	(.26)	26.11	(.30)	26.13	(.26)
	O_2	4.20	(.97)	4.81	(1.27)	5.25	(1.22)	5.11	(.91)
		3.56	(.74)	3.44	(.60)	3.55	(.84)	3.36	(.84)

1969, (3) April through June, 1969, and (4) July through August 1969. Values are given for the surface and bottom waters. Values in parentheses are the sample standard deviations calculated for small sample sizes (less than 30 observations in each sample) by the equation

$$s = \left[\frac{\sum x^2_i - \frac{(\sum xi)^2}{n}}{n - 1}\right]^{1/2}$$

where s is the sample standard deviation, n is the number of observations, and the x's are the values of the observations.

Temperature

Sverdrup et al. (1942) reported that upwelling occurred in the summer months and northward currents prevailed in the winter months along the coast in the Pacific Northwest. These conditions have been observed regularly off the Oregon coast (Rosenburg, 1962). The ocean "seasons" off Newport are clearly seen in Figure 5. October and November are seen as months of transition with moderating temperatures. September is also included in this season, although no temperatures were plotted for that month.

The winter season occurs during December, January, February and March. Strong southerly winds and latitudinal cooling produce a deep, well-mixed surface layer. Cold rains and the resulting excessive runoff often give rise to surface water colder than the

deeper water, as shown for December when the surface water was nearly 2.0°C cooler than the bottom water. This temperature regime was common through the month of February.

Data for April, May and June show the effects of gentle winds and increased solar heating. Surface and bottom waters warmed rapidly, reaching a maximum of 14.5°C near the middle of June. This apparently is not a stable season since rapid temperature fluctuations occurred particularly in May. Sample standard deviations (Table 1) are nearly 2°C for this season.

July and August constitute the upwelling season when strong northerly winds produce a surface current flowing 45° to the right of the wind stress and a net transport of water offshore due to the rotation of the earth (Smith, 1968). Cold water from depths of 200 meters or less well upward to replace the offshore flowing surface waters. The rapid temperature drop in May was very likely due to temporary upwelling, but a subsequent relaxation of wind stress allowed the warming effects to continue through June. The beginning of the season was recorded on BT slides. At 12:45 PDT, June 30, temperatures inside and outside the bight were nearly 14°C at the surface with cold upwelled water lying just below. At the station out of and upstream from the effluent plume the 12°C isotherm was found at 6.0 meters. At 12:50 PDT, July 1, the 12°C isotherm had risen 1.3 meters, requiring an average vertical velocity of about 20 cm

per hour.

Another feature of interest was observed during this upwelling period. Outside the bight, bottom waters were nearly 1°C colder than the bottom waters within the bight, while the outside surface waters were more than 2.0°C warmer than those within, indicating that warm waters inside the bight had been moved or were in the process of moving offshore being replaced by cold upwelled water.

In spite of the seasons described by the water temperatures, each station deviated from the reference outfall station in a somewhat regular manner. The water lying inside the bight appeared to be a well-mixed water mass. Stratification was observed only during the latter half of May. Waves, wind, and tidal action apparently maintained homogeneity. The effluent rising from the outfall did have the effect of producing an upwelling of colder bottom water. As the less dense effluent mixed turbulently at a depth of about ten meters, the resulting mixture rose to the surface. Consequently, the temperatures observed at the station in the effluent plume downstream from the outfall were considerably cooler than at the other stations, except during the upwelling season, when the temperatures at the outfall station were cooler. During the latter season the effluent "puddled" above the diffusers, whereas during the other seasons mixing and dispersion were more rapid at the station in the downstream effluent plume.

Daily temperatures measured from the beach north of Little Creek by Gonor et al. (1970) indicate water in the surf zone exhibits seasonal characteristics also (Figure 9). Rapid fluctuations occurred from day to day and there apparently was a considerable lag time between events occurring in the nearshore zone and the surf zone. The beginning of upwelling season was very abrupt as measured at the outfall station on July 1, but the water in the surf zone remained warm until July 5. This indicates that temperature measurements taken from the beach do not necessarily represent oceanic conditions just offshore.

During the upwelling season, temperatures within the bight were cooler than outside, suggesting that further upwelling occurred due to the northerly wind which "drags" water toward the south, lowering the water level south of Yaquina Head, and allowing subsurface waters to well up on the leeward side of the promontory. High altitude photographs taken on July 16, 1969 also indicated a different type of water in the area just south of Yaquina Head.

Salinity

Pattullo and Denner (1965) found upwelling and river runoff to be the most important processes affecting ocean waters along the Oregon coast. Table 1 indicates that the highest salinity values, over 33.0‰, occurred during the upwelling season. These salinities are

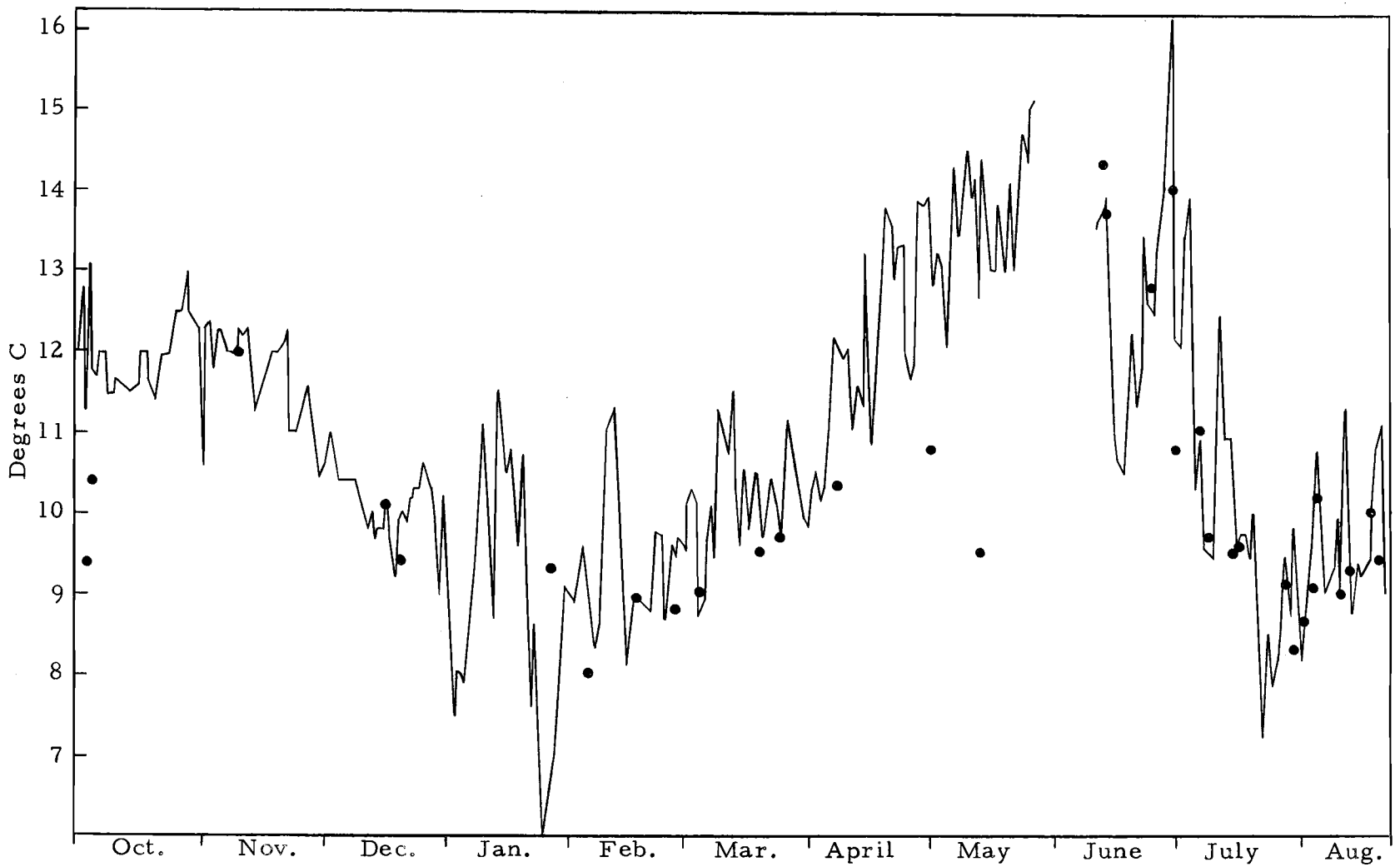

Figure 9. Surf temperatures measured at Agate Beach north of Little Creek (Gonor et al., 1970). Line indicates surface temperatures at the outfall station; dot is outfall surface temperature.

found at a depth of about 80 meters further offshore. The lowest salinities, less than 31.0‰, occurred during the December to March season when rainfall and runoff from coastal streams were at a maximum.

Except during the upwelling season, the highest salinities within the bight were observed at the station located downstream in the effluent plume, because the deeper, more saline waters (welled up from the diffusers) were rapidly advected downstream from the outfall. During the upwelling season currents and mixing were reduced and puddling of the effluent may have allowed dilution of the upwelled water by the less-saline effluent; consequently, the salinities of the outfall during this season were somewhat lower than in the surrounding waters.

Daily salinities measured at Agate Beach, north of Little Creek (Gonor, 1970), showed extreme variations both daily and seasonally (Figure 10). During the winter and spring months, variations were probably due to local runoff and heavy rainfall. The upwelling season was characterized by high salinity and low variability. Similar to the surf zone temperature (Figure 9), high values of salinity (indicating upwelled water) were not measured in this surf area until July 5, four days after upwelling was apparent just offshore.

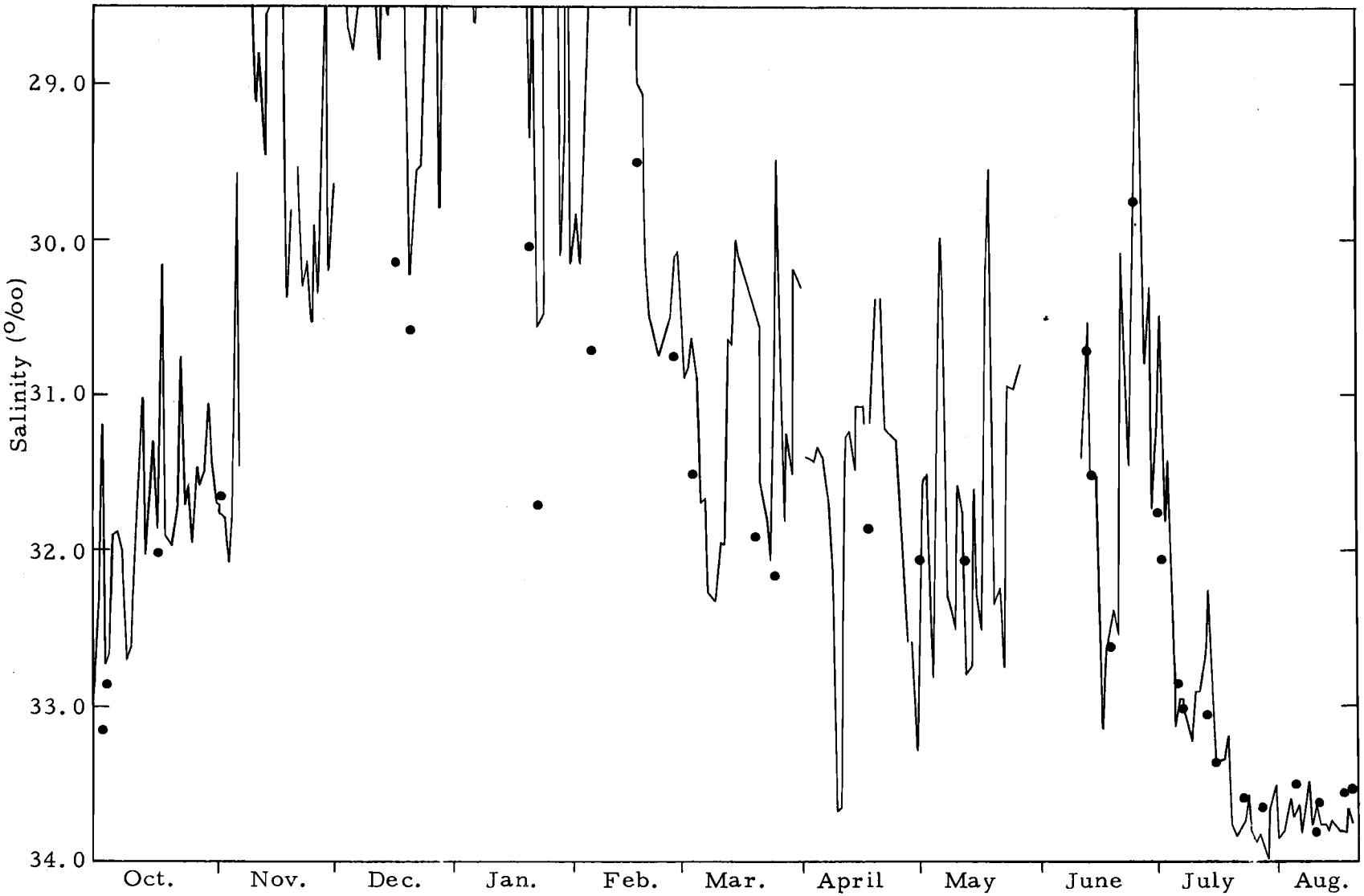

Figure 10. Surf salinities measured at Agate Beach north of Little Creek (Gonor et al., 1970). Line indicates surface salinities recorded at outfall station; dot is outfall surface salinity.

Density

Sigma-t values reached a maximum of about 26.0 during the upwelling season. Water of equal density was found at depths of about 100 meters at stations 50 miles offshore. During the September to November season, density appeared to be influenced by precipitation and runoff. In the December to March season, the lower salinities caused the σt values to be less than 25.0.

Water inside the bight appeared to be more homogeneous with less daily variability than those outside the reef. Deviations were much larger during all seasons beyond the reef. Yaquina Head and the northern Yaquina Bay jetty may shelter the bight from rapid changes which occur outside the reef.

Dissolved Oxygen

The dissolved oxygen content is not a conservative property of sea water because biological and chemical changes can cause large variations in the oxygen content. Physical changes also affect the amount of dissolved oxygen in water, particularly at the surface. Vigorous wave action increases the dissolved oxygen content while warming of the water reduces the amount of dissolved gas the water can contain. Nevertheless, it can be a useful parameter when measuring changes which occur within a water mass and for distinguishing

between water masses. Of value in this study is the surface saturation content which is the theoretical amount of dissolved oxygen that sea water at the surface can "hold" at a particular water temperature.

Throughout the year the dissolved oxygen content was usually found to be equal to or greater than the surface saturation values, except for periods of upwelling. Super-saturation can occur when wave and wind action are vigorous enough to induce increased aeration of the surface water (Green et al., 1967).

During upwelling seasons the upwelled water is much lower in oxygen content. Thus, lower oxygen values characterize the upwelling season. They are much less than the corresponding saturation values plotted in Figure 7. Table 1 indicates that surface waters at the outfall and the downstream effluent plume stations were lower in dissolved oxygen content than waters outside the effluent plume. These oxygen "sags" can be caused by several mechanisms, including interference of the oxygen determination reagents by chemicals in the effluent.

To examine the possible interference of the pulp mill effluent on the determination of dissolved oxygen using the Winkler iodometric method, a series of oxygen measurements were made on known dilutions of effluent and sea water. (No attempt was made to separate the Winkler reagent interference and the actual chemical oxygen demand of the effluent, although it was assumed that the former was

of greater magnitude.) A sample of the effluent was obtained from the Georgia-Pacific pulp mill in Toledo, Oregon, and a volume of sea water was collected at the Marine Science Center in Newport during flood tide. A large number of dilutions were chosen, partly to observe scatter in the data, and partly to look at detail. For each dilution three sample bottles were prepared. One bottle contained only sea water while the other two had a specific volume of effluent introduced just prior to adding the sea water, thus giving two bottles with the same dilution. Each of the three bottles were "pickled" immediately. The dilutions ranged from 1:10 to 1:20,000 by volume. Four hours after pickling, the sample containing only sea water and one diluted sample were acidified and titrated. After 24 hours the second diluted sample was acidified and titrated to determine any slow reactions occurring between the effluent and the Winkler reagents. The results are given in Table 2.

The data indicated that a decrease of the oxygen value occurred at the dilution of one part effluent in 600 parts sea water for both the four-hour delay and the 24-hour delay. An apparent decrease in oxygen values in the 24-hour delay over those of the four-hour delay indicated that some slow rate reactions did occur.

James (1970) determined the dilution values of effluent-contaminated surface waters within the bight during the summer seasons when dilution is expected to be at a minimum. He found that

Table 2. Dissolved oxygen content of effluent-sea water dilutions.

Dilution	Non-diluted sea water standard, 6.14 ml/l dissolved oxygen			
	4 Hours ml/l	24 Hours ml/l	Sample minus standard 4 hr	Sample minus standard 24 hr
1:20,000	6.15	6.15	.01	.01
1:10,000	6.18	6.16	.04	.02
1:5,000	6.20	6.10	.06	- .04
1:2,500	6.10	6.15	- .04	.01
1:2,000	6.16	6.10	.02	- .04
1:1,000	6.14	6.04	.00	.10
1:800	6.17	6.08	.03	- .06
1:600	6.11	6.03	- .03	- .11
1:500	6.11	6.13	- .03	- .01
1:400	6.06	6.00	- .08	- .14
1:300	6.08	5.98	- .06	- .16
1:200	6.02	5.94	- .12	- .20
1:100	6.00	5.84	- .14	- .30
1:50	5.88	5.78	- .26	- .36
1:25	5.64	5.63	- .50	- .51
1:10	4.94	4.72	-1.20	-1.42

on an average summer day, the surface water directly over the diffusers had a dilution of about 1:850. If we assume that this is near the minimum dilution encountered throughout the year, the Winkler iodometric method for oxygen determination can be considered valid to at least several hundredths of a milliliter of dissolved oxygen per liter of sample. The oxygen sags seen at the surface for outfall and downstream effluent plume stations were probably due to the upwelling of bottom water when the fresh water effluent rose to the surface bringing up water of lower dissolved oxygen content with it.

The Stepwise Multiple Regression Procedure

Ocean currents are one of the most important of all ocean variables. A thorough knowledge of the currents in the bight would allow inferences to be made of the influence that waste effluents would have on the beach or at some position "downstream." Typical marine disposal systems of the past have been constructed with little concern for the effects of the effluent once it has left the diffuser pipes. Recently, however, beach pollution and the staggering load of effluents to be discharged has prompted a more careful review of the receiving waters.

A major goal of this study was to determine how physical factors of the Oregon coast affect the nearshore waters. In particular the year-long observation program allowed an examination of these factors during the winter when practically no measurements of any type had been conducted in that nearshore area. Each current measured can be thought of as the resultant of a number of different and usually independent current producing forces. These current producing forces may be hidden or sometimes only implied within a group of observations. Therefore, the choice of analysis was the multiple regression approach to gain a knowledge of the individual and the joint effects produced by the current producing components.

The Statistics Department at Oregon State University maintains a library of statistical routines which are available for researchers at

the University. One program, referred to as *Step, is a step-wise multiple linear regression analysis program developed primarily on the work of Efroymsen (Ralston and Wilf, 1960). As the name implies, the program performs a regression of many independent variables on one dependent variable using a linear, least-squares approach to reduce the sum of squares of deviations about the regression line to a minimum. Of particular interest is a parameter known as r^2, or the regression coefficient, which is equal to the ratio of the reduction in the sum of squares of deviations obtained by using a linear fit to the total sum of squares of deviations about the sample mean, or $r^2 = \Sigma (\hat{V}i - \bar{V})^2 / \Sigma (Vi - \bar{V})^2$. The value of r^2 can be interpreted as the proportion of the variance about the linear model which is explained by regression. Multiplying by 100 expresses r^2 as the percentage of explained variance.

The general form of the regression equation used in the study was

$$V = B_o + B_1 x_1 + B_2 x_2 + \ldots B_n x_n + \epsilon$$

where V is the predicted current vector and the B's are constant coefficients determined by the regression program. The x's are values of the independent variables, or current producing forces, and ϵ is the error or residual term. The regression equation may be thought of as a linear equation of several variables where B_o is the Y intercept and the x's describe the slope of the line.

*Step computes the values of B_o and B_i in the regression equation with an accompanying F value for determining the significance of the regression for each coefficient. The F value is computed from the ratio of the mean square due to regression (MS_R) to the mean square due to residual variation (s^2), or $F = MS_R/s^2$. It can be shown statistically that the expected value of MS_R and s^2 (Draper et al., 1966) are

$$E(MS_R) = \sigma^2 + B_i^2 \sum_{j=1}^{n} (x_{ij} - \bar{x}_i)^2$$

$$E(s^2) = \sigma^2$$

The ratio MS_R/s^2 can be compared with the tabulated F (one and n-2 degrees of freedom) at the 100 $(1 - \alpha)$% level to determine whether B_i can be considered zero, which indicates that the coefficient is not useful in predicting values of V.

The x's must be linear functions of V requiring a conversion of the basic data into linear functions of V. How well the variable describes the current can then be determined by the regression analysis. The particular effect each variable has on the current is not well known, especially in shallow waters. Therefore, a consideration of a number of expressions for each variable was required. After running an analysis with all expressions included, those which were insignificant were removed. In this manner the "best" expressions for the regression equation were derived from a number of possible expressions.

Nearshore Currents

A computer program was written to obtain the linearized current producing variables used in the regression analysis. The meaning of each numbered variable is given in Table 3.

Table 3. Current-producing variables used in the regression analysis.

1.	Tidal component.
2.	Wave component derived from Longuet-Higgins' equations.
3.	Wave component according to Stokes' theory.
4.	Wave component based on a selection between 2 and 3 above, depending on the wave length and depth of water.
5.	Wind speed component for winds observed during the observation hour.
6.	Wind speed component for winds observed during the hour prior to the observation.
7.	Wind speed component for winds observed two hours before the observation.
8.	Wind stress term based on the winds measured during the hour of observation.
9.	Wind stress term based on the winds measured during the hour prior to the observation.
10.	Wind stress term based on winds measured during the period two hours before the observation.
11.	Average of 8 and 9 above.
12.	Average of 8 and 10.
13.	Average of 9 and 10.
14.	Average of 8, 9 and 10.
15.	Weighted average of 8 and 9.
16.	Weighted average of 8, 9, and 10.
17.	Second weighted average of 8, 9, and 10.
18.	Current vector to be predicted.

All 18 variables were initially included in computations for the outfall and Big Creek stations. Those variables with small contributions to the reduction of variance were then removed; the program was

run again using the remaining variables as well as new variables obtained by multiplication of the remaining variables by themselves. Heightened effects produced by interactions of two variables were examined by the intermultiplication of independent variables. The current components at the outfall and Big Creek were added to the variables used in the jetty and Yaquina Head analysis, respectively, to determine the effect of the known current flow away from the boundaries imposed by the jetty and Yaquina Head.

For each location the variables which contributed to a reduction of variance are listed in Tables 4, 5, 6 and 7 with the value of r^2, the computed F value, and the tabulated F value at the 95% and 99% level. If the computed F value exceeds the tabulated F value we can be 95% or 99% confident, depending on which F value is exceeded, that the addition of the variable is significant in reducing the variance. The computer program allows the user to choose an F value below which the variable is deleted from the analysis. The value of 0.001 was chosen to allow an evaluation of each variable's relative contribution to the reduction of the variance, even though that F level was much too low to be considered significant.

The dominant effect of the wind at the outfall station is readily shown by the regression analysis. In the north-south direction the wind contributed all the significant reduction of variance. Other parameters are insignificant according to the computed F distribution.

Table 4. Variables contributing to the reduction of variance of observed currents at the outfall station.

	r^2	F	95% and 99% Tabular F
North-south components			
All 18 variables			
6. Winds of the previous hour	56.9%	122.7	4.0, 7.0
8. Wind stress term for the present hour's wind	0.7	1.4	" "
3. Stokes' wave transport	0.6	1.3	" "
5. Winds of the present hour	0.5	1.1	" "
4. Selection of Stokes' and Longuet-Higgins' wave transport	0.3	0.5	" "
10. Wind stress term for two hours previous winds	0.3	0.5	" "
1. Tidal component	0.8	0.2	" "
7. Winds of two hours previous	0.5	0.1	" "
2. Longuet-Higgins' wave transport	0.0	0.0	" "
Remaining variables and their interactions			
6. Winds of the previous hour	56.9	122.7	4,0, 7.0
1x6. Interaction of winds of previous hour and the tidal component	1.3	2.8	" "
7. Winds of two hours previous	0.5	1.3	" "
1. Tidal component	0.5	1.1	" "
East-west components			
All 18 variables			
6. Winds of the previous hour	26.6	33.8	4.0, 7.0
1. Tide	4.3	5.8	" "
9. Wind stress term of the previous hour's wind	2.6	3.6	" "
7. Winds of the two hours previous	2.1	2.9	" "
5. Winds of the present hour	0.9	1.2	" "
10. Wind stress term of two hours previous wind	0.5	0.7	" "
3. Stokes' wave transport	0.2	0.3	" "
2. Longuet-Higgins' wave transport	0.6	0.8	" "
4. Selection of Stokes' and Longuet-Higgins' wave transport	0.6	0.8	" "
14. Average of the three wind stress terms	0.0	0.1	" "
Remaining variables and their interactions			
6. Winds of the previous hour	26.6	33.8	4.0, 7.0
5. Wind of the present hour	4.6	6.6	" "
1. Tide	4.3	5.8	" "
7. Wind of the two hours previous	2.1	2.9	" "
3x6. Interaction of winds of the previous hour and Stokes' wave transport	1.3	1.8	" "
1x3. Interaction of the tide and Stokes' wave transport	0.9	1.3	" "

The north-south current velocity component can be estimated by $Vns = 0.74 + 0.59\ W_1$, where W_1 is the wind of the previous hour. The east-west current velocity component appears to be a result of the wind and the tide. The predictor equation in the east-west direction is given as $Vew = -1.91 + 0.78\ W_1 + 1.18\ T + 0.43\ W_o$, where W_1 is wind of the previous hour, T is the tide, and W_o is the wind of the present hour.

It is interesting to note that in the absence of current producing parameters the resultant of the north-south and east-west current vectors indicates a flow toward west by northwest, or $\tan^{-1}(0.74/1.91) = 291^{o}$, with a velocity of 2.1 cm/sec.

The currents at Big Creek are also dominated by the wind but unlike the outfall location, the winds of the present hour do affect the current. The contributions of the parameters, tide and waves, are similar at both locations. The influence of Yaquina Head on the wind field at Big Creek is not known but the effect could be enough to account for the reduced r^2 values at the Big Creek station.

For the north-south current velocity components the regression equation is $Vns = 2.07 + 0.38\ W_o$, where W_o is wind of the present hour. For the east-west current components the calculated prediction equation is $Vew = 0.92 + 0.29\ W_o$. Although the tide and perhaps several other terms do appear to contribute to the current, their contributions, as indicated by the F value, are too small to warrant

Table 5. Variables contributing to the reduction of variance of observed currents at the Big Creek station.

	r^2	F	95% and 99% Tabular F
North-south components			
All 18 variables			
5. Wind of the present hour	32.2%	36.1	4.0, 7.0
2. Longuet-Higgins' wave transport	2.6	3.0	" "
8. Wind stress term of present hour's wind	1.5	1.7	" "
1. Tide	0.5	0.6	" "
11. Average wind stress term for winds of present and previous hour	0.4	0.5	" "
3. Wave transport (Stokes')	0.3	0.3	" "
6. Wind of previous hour	0.1	0.1	" "
7. Wind of two hours previous	0.0	0.0	" "
Remaining variables and their interactions			
5. Wind of the present hour	32.2	36.1	4.0, 7.0
1x5. Interaction of tide and wind of present hour	1.1	1.2	" "
1. Tide	0.8	0.9	" "
1x2. Interaction of tide and Longuet-Higgins' wave transport	0.4	0.4	" "
2x5. Interaction of Longuet-Higgins' wave transport and wind of present hour	0.3	0.3	" "
2. Longuet-Higgins' wave transport	0.2	0.2	" "
East-west components			
All 18 variables			
5. Wind of the present hour	22.2	21.7	4.0, 7.0
1. Tide	2.8	2.8	" "
15. A weighted wind stress term	1.5	1.5	" "
2. Longuet-Higgins' wave transport	0.5	0.5	" "
10. Wind stress term of previous two hours	0.3	0.3	" "
6. Winds of the previous hour	0.2	0.2	" "
7. Winds of two hours previous	0.1	0.1	" "
11. Average of wind stress term of present and previous hour's winds	0.1	0.1	" "
3. Stokes' wave transport	0.1	0.1	" "
Remaining variables and their interactions			
5. Wind of the present hour	22.2	21.8	4.0, 7.0
1. Tide	2.8	2.8	" "
2x5. Interaction of Longuet-Higgins' wave transport and winds of present hour	1.7	1.7	" "
1x5. Interaction of tide and wind of present hour	0.1	0.7	" "
1x2. Interaction of tide and Longuet-Higgins' wave transport	0.0	0.4	" "
2. Longuet-Higgins' wave transport	0.0	0.0	" "

including them in the prediction equation at the 95% confidence level.

In the absence of winds the resultant of the east-west and north-south current vectors is a current flowing to the north northeast, or $\tan^{-1}(0.92/2.07) = 024^{o}$, with a velocity of 2.3 cm/sec.

The 18 basic variables used in the analysis for the outfall and Big Creek locations were not used for either the Yaquina Head or the jetty stations. The majority of these terms were expressions for the wind, and it was assumed that the wind would have even less effect at these two areas because of the proximity to Yaquina Head and the jetty, respectively. Two new terms were added which were thought to influence the currents at these locations. The north-south and east-west components of the Big Creek and outfall stations could "force" a current at the boundary areas by creating a hydraulic difference, and thus were added to the analysis. Additionally, because of the reduced number of observations at these locations (about 50 at each location), fewer variables had to be used to obtain a statistically meaningful result. As the number of variables approaches the number of observations, the r^2 value departs from an indicator of the reduction of variance and begins to indicate how well the regression line fits the regression equation. Obviously, with n variables and n observations, the regression equation will have n coefficients, which will then pass through all observation points exactly with an r^2 value of 100%.

The use of the computed prediction equation (Table 6) for

Table 6. Variables contributing to the reduction of variance of observed currents at the Yaquina Head station.

		r^2	F	95% and 99% Tabulated F
	North-south components			
A.	North-south current component at Big Creek	10.2%	6.1	4.0, 7.1
6.	Wind of previous hour	3.0	4.9	" "
1.	Tide	5.2	3.2	" "
2.	Longuet-Higgins' wave transport	3.9	2.5	4.1, 7.2
3.	Stokes' wave transport	2.8	1.7	" "
4.	Selection between Stokes' and Longuet-Higgins' wave transport	2.1	1.3	" "
5.	Wind of present hour	1.4	0.9	" "
B.	East-west current component at Big Creek	0.2	0.1	" "
7.	Winds of previous two hours	0.1	0.1	" "
	East-west components			
6.	Wind of previous hour	5.3	3.2	4.0, 7.1
A.	North-south current component at Big Creek	4.6	2.6	" "
4.	Selection between Longuet-Higgins' and Stokes' wave transport	4.1	2.6	" "
5.	Wind of present hour	1.7	1.0	" "
7.	Wind of previous two hours	0.5	0.3	" "
1.	Tide	0.5	0.3	4.1, 7.2
B.	East-west current component at Big Creek	0.5	0.3	" "
2.	Longuet-Higgins' wave transport	0.0	0.0	" "
3.	Stokes' wave transport	0.0	0.0	" "

Yaquina Head may not be entirely justified since only the Big Creek north-south current component variable is significant in the reduction of variance according to the F level test. Furthermore, no variable of the east-west components exceeded the tabulated F value. Wetz (1964) suggested that for an equation to be regarded as a satisfactory predictor, the F value should not only exceed the tabulated value but should be about four times as large. On this basis no equation can be used at Yaquina Head for these data. However, if the constant terms, B_o, can be used as an estimate of currents in the absence of the examined current producing forces, the resultant of the east-west and north-south current vectors is a residual current flowing towards the south southwest.

In both the north-south and east-west directions the winds of the previous hour have negative coefficients (-0.3 and -0.9, respectively) indicating that the current response may be due to the return flow of water as it is pushed against the Yaquina Head boundary. Since the Big Creek north-south current component apparently affects the east-west flow, the Yaquina Head east-west current is probably a form of hydraulic flow rather than one driven by the wind, waves or tide.

The currents at the jetty are similar to those at Yaquina Head possibly because of the boundary conditions. The observed currents at both stations are not particularly correlated with the measured parameters (Tables 6 and 7). Only one variable, the north-south

Table 7. Variables contributing to the reduction of variance of observed currents at the Jetty Station.

		r^2	F	95% and 99% Tabulated F
	North-south components			
C.	North-south current component at outfall	23.3%	13.6	4.1, 7.3
2.	Longuet-Higgins' wave transport	5.3	3.3	" "
3.	Stokes' wave transport	3.4	2.1	" "
7.	Wind of previous two hours	2.8	1.7	" "
1.	Tide	0.7	0.4	" "
4.	Selection between Longuet-Higgins' and Stokes' wave transport	0.4	0.2	" "
D.	East-west current component at outfall	0.2	0.1	" "
6.	Wind of the previous hour	0.0	0.0	" "
5.	Wind of the present hour	0.0	0.0	" "
	East-west components			
1.	Tide	7.3%	3.6	4.1, 7.3
7.	Wind of previous two hours	6.2	3.2	" "
C.	North-south current component at outfall	2.6	1.3	" "
6.	Wind of previous hour	2.4	1.2	" "
3.	Stokes' wave transport	2.4	1.2	" "
2.	Longuet-Higgins' wave transport	0.7	0.3	" "
4.	Selection between Longuet-Higgins' and Stokes' wave transport	1.1	0.5	" "
5.	Wind of the present hour	0.7	0.3	" "
D.	East-west current component at outfall	0.4	0.2	" "

current component at the outfall, was significant in explaining the north-south current component at the jetty. Hydraulic flows could dominate the currents at this site and thus mask the effects of the measured variables. The F value for the outfall north-south current component variable is considerably more than the tabulated F value. The prediction equation is Vns = -2.6 + 0.1 [0 Cns], where [0 Cns] is the north-south current component at the outfall. Therefore, an observation of the outfall current is required in order to predict the jetty current, which reduces the usefulness of the equation.

None of the variables appear to be significant in explaining the east-west current at the jetty, although the F level for the tide nearly approaches the tabulated F value. In the absence of current producing forces the east-west current is computed to flow to the west at 3.8 cm per second. The resultant of the east-west and north-south current vectors is a current flowing to the west at 8.0 cm per second, or $\tan^{-1}(-2.6/-7.6) = 251^{\circ}$.

Wind Velocity Versus Current Direction

Throughout the period of observation a deviation between the surface current direction and the current direction at two meters was noted. The deviation was conveniently measured using a three-armed protractor when the 35 mm photographic transparencies of dye paths were projected on a screen. The center of the protractor was placed

over the image of the anchored float. One arm was then placed along the line of green dye emitted from the anchored marker while a second arm extended to the drifting float. The angle subtended was then recorded as the deviation of the current direction at two meters from the surface current direction. The deviations ranged from zero to 180°, although the averages at the outfall and Big Creek were 6.4 and 0.6°, respectively. At both locations the average current direction at two meters was slightly to the left of the average surface current direction. The speeds of the two currents could not be compared, as no value for the surface current speed could be obtained. (The dye on the surface dispersed rapidly and the beginning of the dye trail could not be accurately determined.)

In the preceding analysis of the currents and their possible causal agents, the wind was the dominant component in explaining the observed current vectors. In many instances the current direction alone can be useful in predicting the course of a parcel of water or a tracer substance within the water. Winds at the Big Creek location appeared to be affected by the promontory, Yaquina Head. The outfall location received nearly equal exposure from all wind directions.

Figures 11, 12 and 13 pertain to the outfall location only. Figure 11 is a plot of the deviations (in degrees) of the current direction at a depth of two meters from the previous hour's wind direction versus the wind speed. Figure 12 is a plot of the wind speed versus

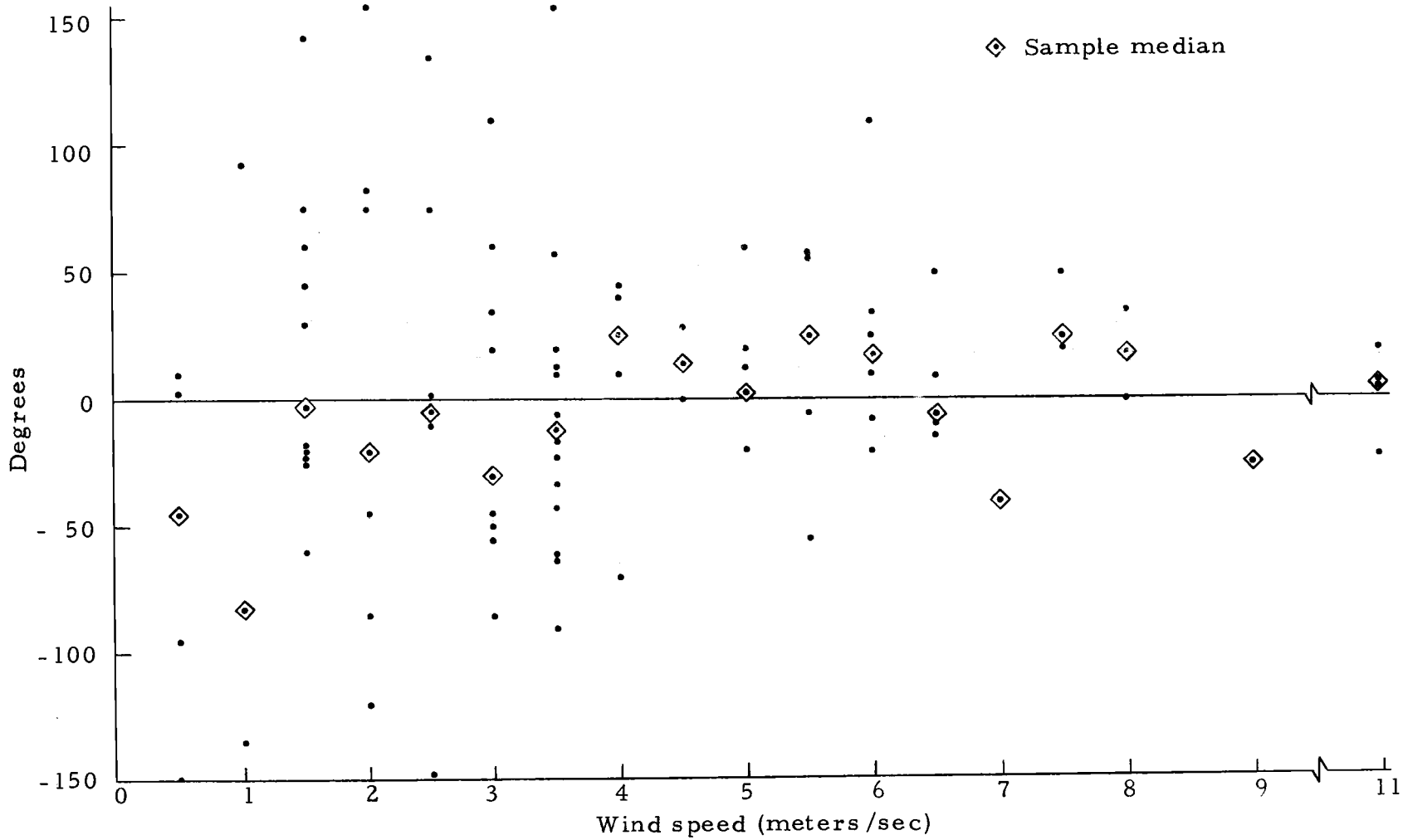

Figure 11. Deviations of the current at a depth of two meters, from the previous hour's wind direction. Positive angles indicate the current flows to the right of the wind direction. (93 observations)

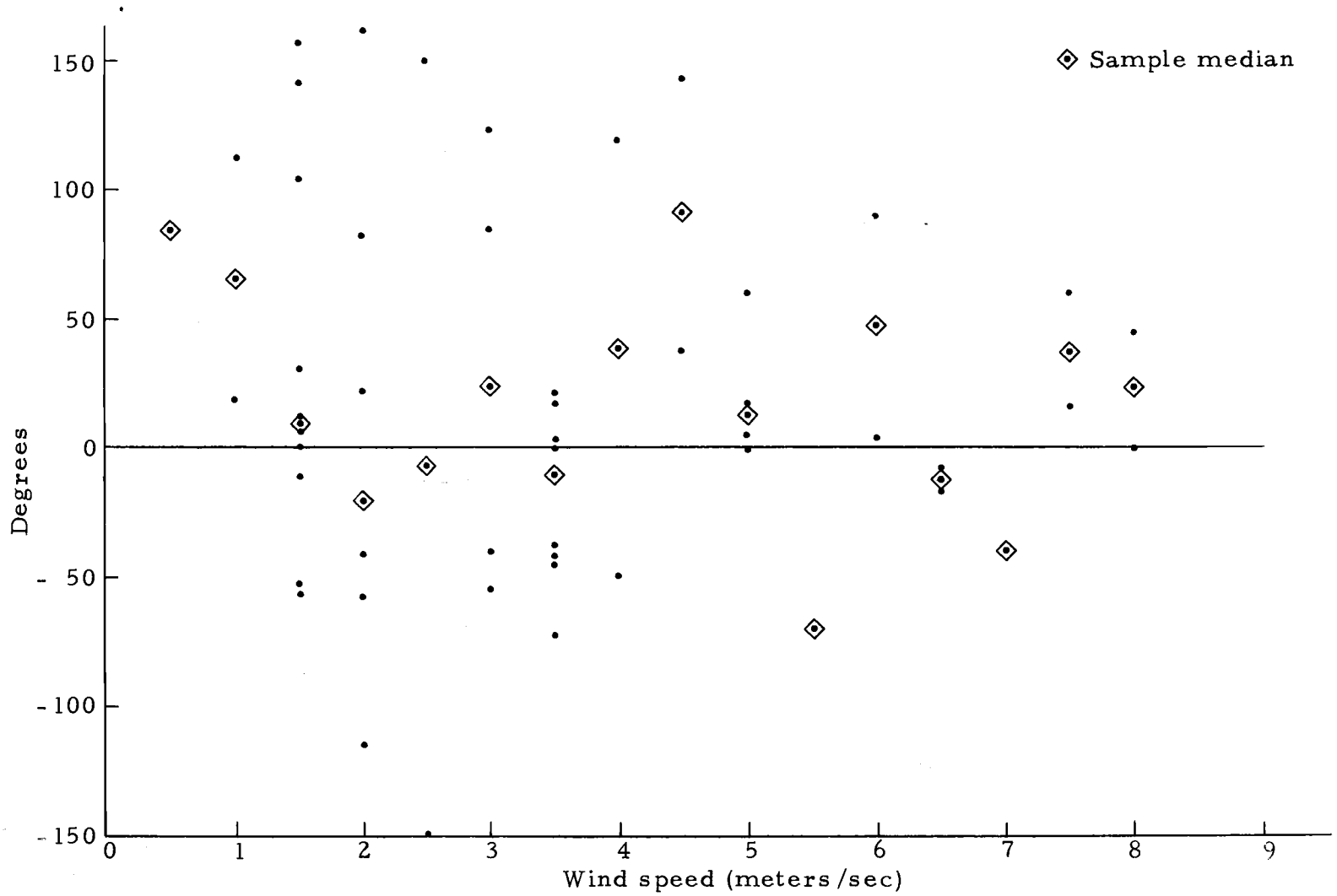

Figure 12. Deviations of the surface current from the previous hour's wind direction. Positive angles indicate the current flows to the right of the wind direction. (57 observations)

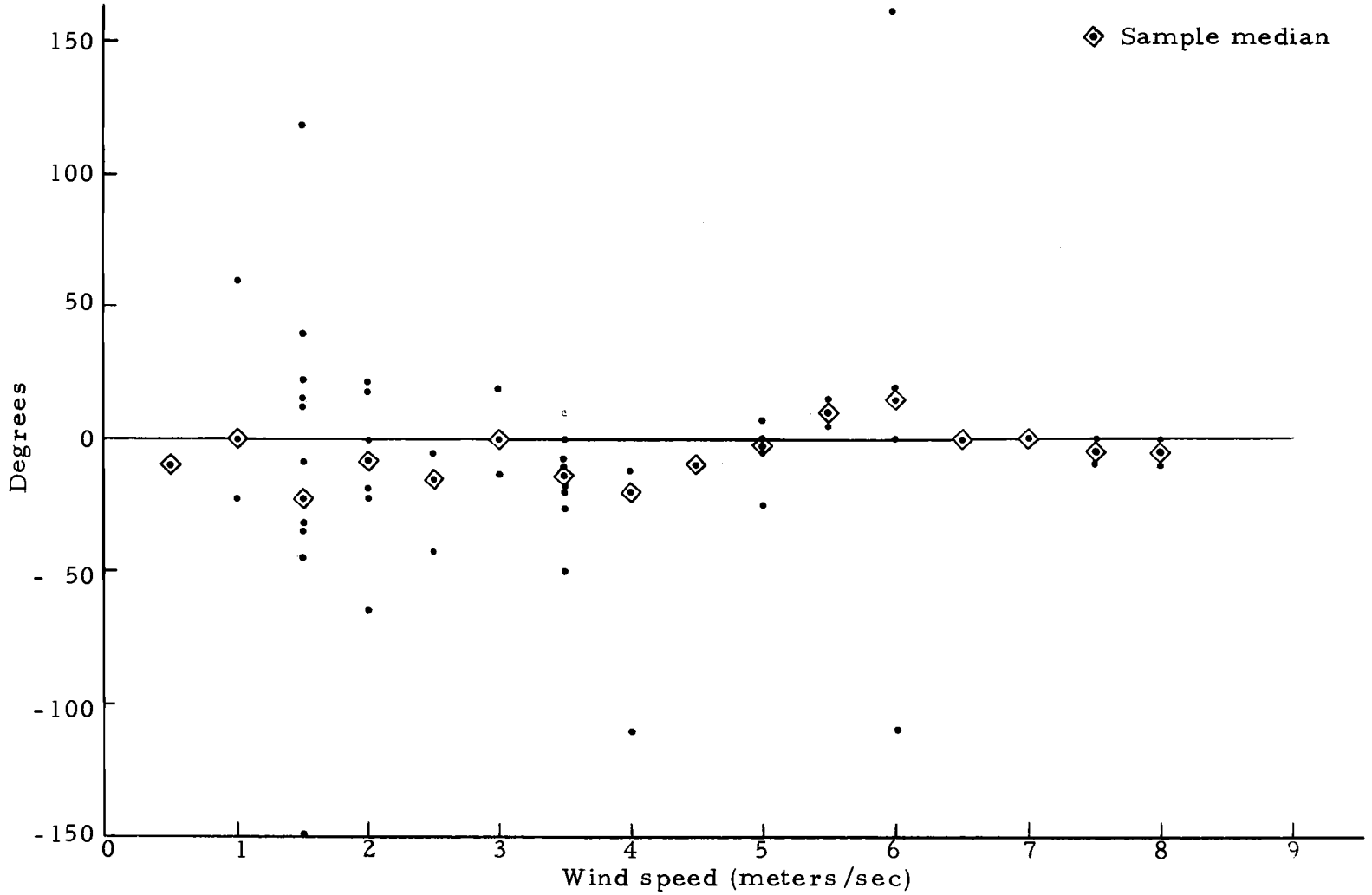

Figure 13. Deviations of the current direction at six feet from the surface current. Positive angles indicate the surface current flows to the left of the current at two meters.

the deviation of the surface current direction from the previous hour's wind direction. Both plots show much variability, showing both real variance and measurement errors. Some points suggest that the recorded direction may have been the reciprocal of the actual direction since 180° deviations were recorded even at higher wind velocities. Each measurement of current direction was subject to this error, as the airplane pilot occasionally flew the plane in a direction opposite to the direction of windflow when the recording was being made during strong winds. (This maneuver allowed a slower ground speed and thus more time for observation.) In addition to the possible error in the observation each wind direction obtained from the anemometer was accurate only to ± 22-1/2°, as discussed previously.

The median of the direction deviations for each wind speed is indicated on each plot. Median values of the current at two meters for wind speeds of less than 3.6 meters per second are negative (i.e., left of the direction of wind flow). At wind speeds greater than 3.6 meters per second, values are predominantly positive (to the right of the direction of wind flow) but within 25° of zero deviation. This would indicate that the current direction at a depth of two meters is either parallel or slightly to the right (less than 25°) of the wind flow. The points at wind speeds of 0.5 and 1.0 meters per second appear to be unlike the other values because of the large variances and large negative median values.

Figure 11, showing deviations of the current direction at two meters from the direction of wind flow, is similar to Figure 12 in several respects. Median values of 0.5 and 1.0 meters per second are different from the "trend" of successive median values (i.e., the median values center around zero), although the number of points is small. Median values for wind speeds above 6.0 meters per second are nearly identical; they approach zero deviation. Deviation values for wind speeds of 1.5 to 5.5 meters per second are quite similar except for greater variability seen in the surface current deviations. Greater variability is expected in the surface layer, probably because it is subject to more rapid short term variations in wind direction at these moderate wind speeds.

Figure 13 is a plot of the wind speed versus the deviation of the surface current direction from the current direction at a depth of two meters. The deviation values are independent of the accuracy of wind direction measurement because the deviation accuracy was dependent only upon the angle measurement taken from the projected photographic transparency. Considerable variation occurs especially at low wind speeds. Surface currents appear to flow to the right (negative) of the current at two meters at wind speeds of less than 4.5 meters per second. When the wind is greater than 5.0 meters per second the deviations are positive (the surface current flows to the left of the current direction at two meters). Deviations approach zero

for winds above 6.5 meters per second. The two large negative values at 4.0 to 6.0 meters per second occurred just before the onset of upwelling when a distinct thermocline was observed. In each case the surface water was moving offshore while the water at two meters was moving towards the south. It is of particular interest that only one of 19 observations during the upwelling season (June 30 to August 19) produced a positive deviation. Twenty-six of 42 observations during the rest of the year were positive. Sample sizes are too small to separate the four seasons, but these data suggest that during the upwelling season surface drift is slightly to the left of the current at two meters and that for the rest of the year the majority of surface currents are to the right of or parallel to the current at two meters.

Wind Speed Versus Current Speed

The r^2 value is highest for the north-south outfall regression equation and is due almost entirely to the wind. The most basic relationship can be expressed as Vns = 2.28% of the wind speed. The percentage, 2.28%, is also known as the wind factor (k) based on the assumption that a linear relationship exists between the current velocity and the wind velocity.

Many researchers have attempted to determine a value for k. Typical values for surface waters (depths to five meters) range from about 1.0% to over 4% (Tomczak, 1964). Many of the higher values

were found using drift cards. Karwowski (1963) states that doubling the wave height can triple the velocity indicated by drift cards. Therefore, drift cards are probably not suitable for determining currents in areas of large waves. Careful studies usually show a wind factor of about 2% to 3%. Ekman (in Tomczak, 1963) reported a factor of 1.85% using current measurements from an anchored ship. For estimating wind-driven currents over the continental shelf, Bretschnieder (1967) presented the formula of Vns = 0.00296 $(\text{Depth})^{1/6}$ (wind speed in meters/sec). For a depth of ten meters, $(\text{depth})^{1/6}$ is approximately 0.5 and the formula gives the velocity of the current as 2.8% of the steady-state winds. Rossby and Montgomery (1935) concluded from the theory of fluid dynamics that the wind-current ratio varied from 2.27% to 3.17% with the lower value occurring at increasing latitudes and wind speeds.

Many authors have suggested that a critical wind speed exists, beyond which there is a step change in the energy transfer rate from the wind to the ocean surface. This critical speed is thought to be about six or seven meters per second (Munk, 1947). To examine this data for a critical wind speed the north-south current component at the outfall station was plotted versus the present hour's wind component (Figure 14). The least squares fit given by the regression analysis is shown by the broken line. For winds from the north (negative values) the line appears to predict the current well.

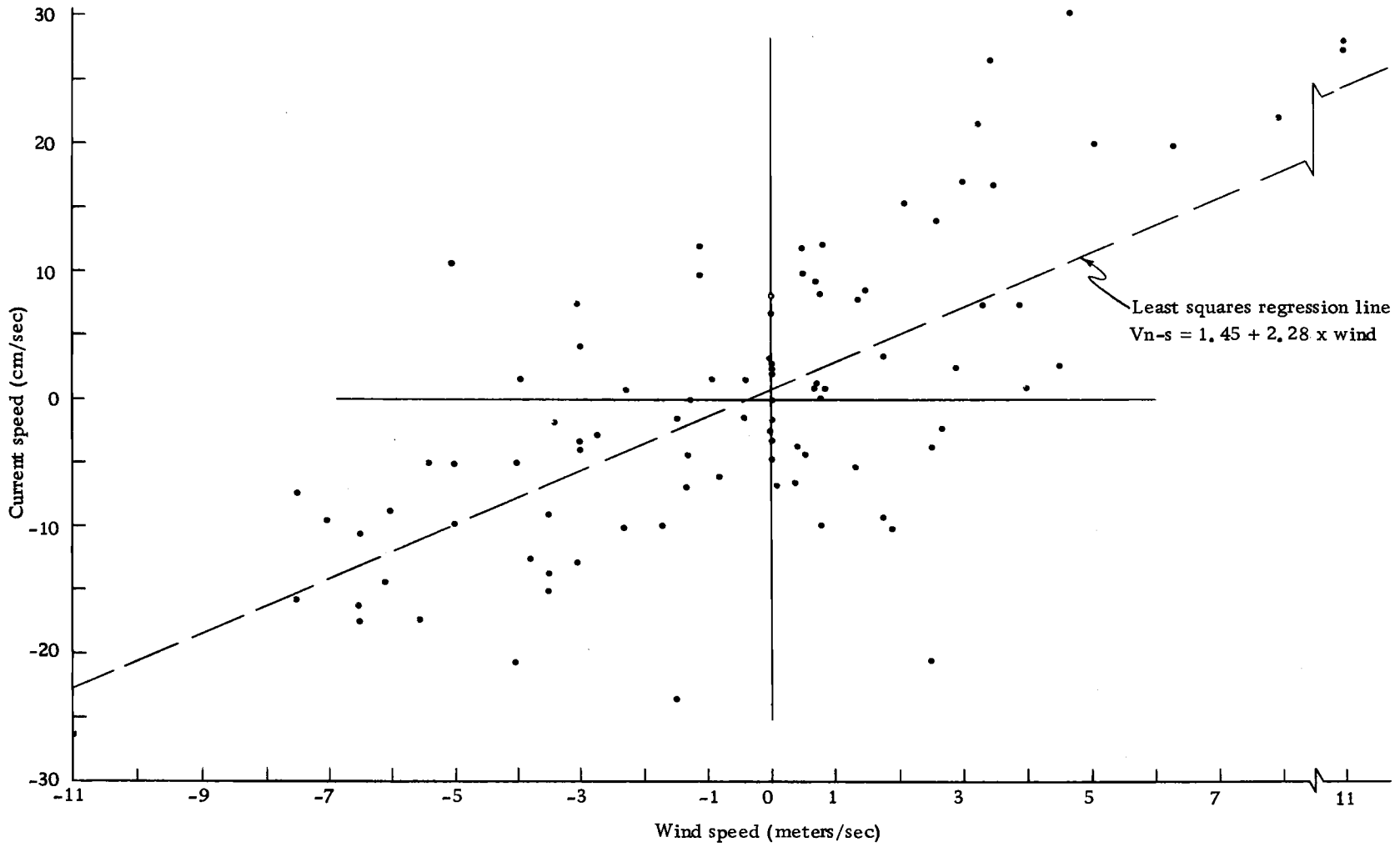

Figure 14. The north-south current component at the outfall station versus the north-south component of the previous hour's wind. Positive values indicate the flow is to the north.

However, winds from the south (positive values) with speeds up to about five meters per second appear to underestimate the currents. At wind speeds above five meters per second the current increases less rapidly with increasing wind speeds. This result tends to confirm Munk's conclusion that there is a critical wind speed. However, the critical wind speed only occurs during winds blowing to the north for this particular location. At stations within the bight topographic features probably play an important role. Currents and winds flowing to the south are not particularly disrupted but the currents moving to the north are at least partially disrupted by the entrance of Yaquina Bay and the north jetty and therefore cannot be considered steady state as they move past the outfall location.

The effect of topography can also be seen in Figure 15, a plot of the north-south current vector versus the north-south wind component at the Big Creek station. Currents flowing to the north appear to be hindered by Yaquina Head and are consequently slow, being predominantly less than 3 cm/sec. Southward flowing currents are more evenly distributed with a break again at wind speeds of five meters per second. However, there is still much variability in these data.

Longshore Currents

Longshore currents are assumed to be generated by the

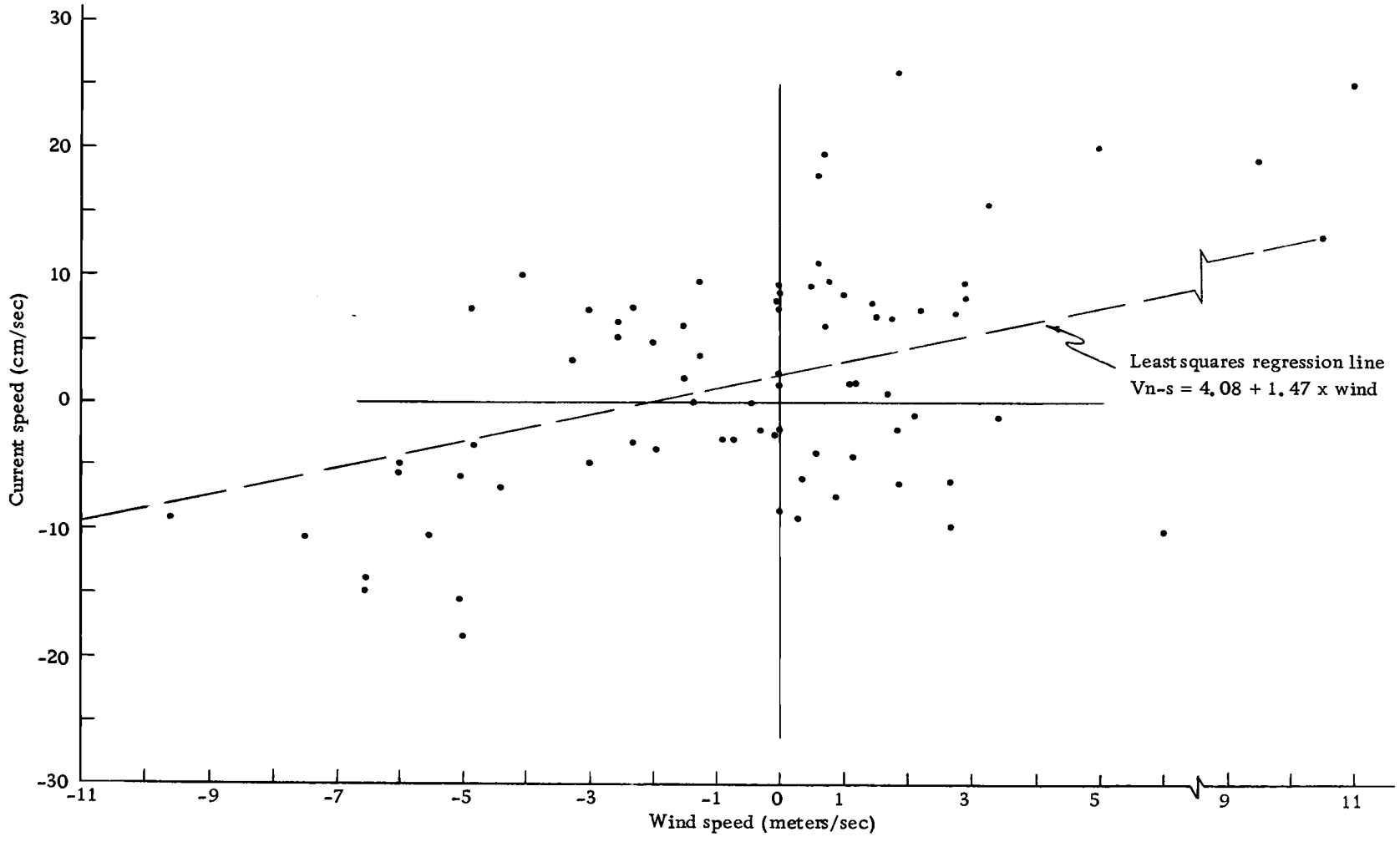

Figure 15. The north-south current component at the Big Creek station versus the north-south component of the present hour's wind. Positive values indicate the flow is to the north.

longshore component of momentum in the breaking waves. Large waves were measured throughout the year at Newport but were more frequent during the winter season (Figure 16). Although a relationship between the waves and the longshore current has been recognized for many years, a thorough analysis did not appear until a comprehensive study was made by Putnam et al. (1949). Putnam's results were modified by Inman and Quinn (1951) and became one of the accepted methods of predicting longshore currents. However, many subsequent field and laboratory observations did not agree with Putnam's equation. A number of investigators attempted different methods for predicting the longshore current velocities. Many of these methods were simply refinements of Putnam's method which assumes that an energy flux is imparted into the surf zone from a solitary wave form. Some methods have assumed a conservation of mass (Brunn, 1963). Galvin (1967), reviewing existing longshore current theory and data, concluded that a proven prediction of longshore currents did not exist and that reliable data on longshore currents was not available for a wide range of current flows. He also found that most data available agreed partially with most equations. According to Galvin, "at present the best approach to a meaningful prediction of longshore current velocity is through empirical correlation of reliable data" (p. 303).

Sonu et al. (1967) used a multiple linear regression analysis of

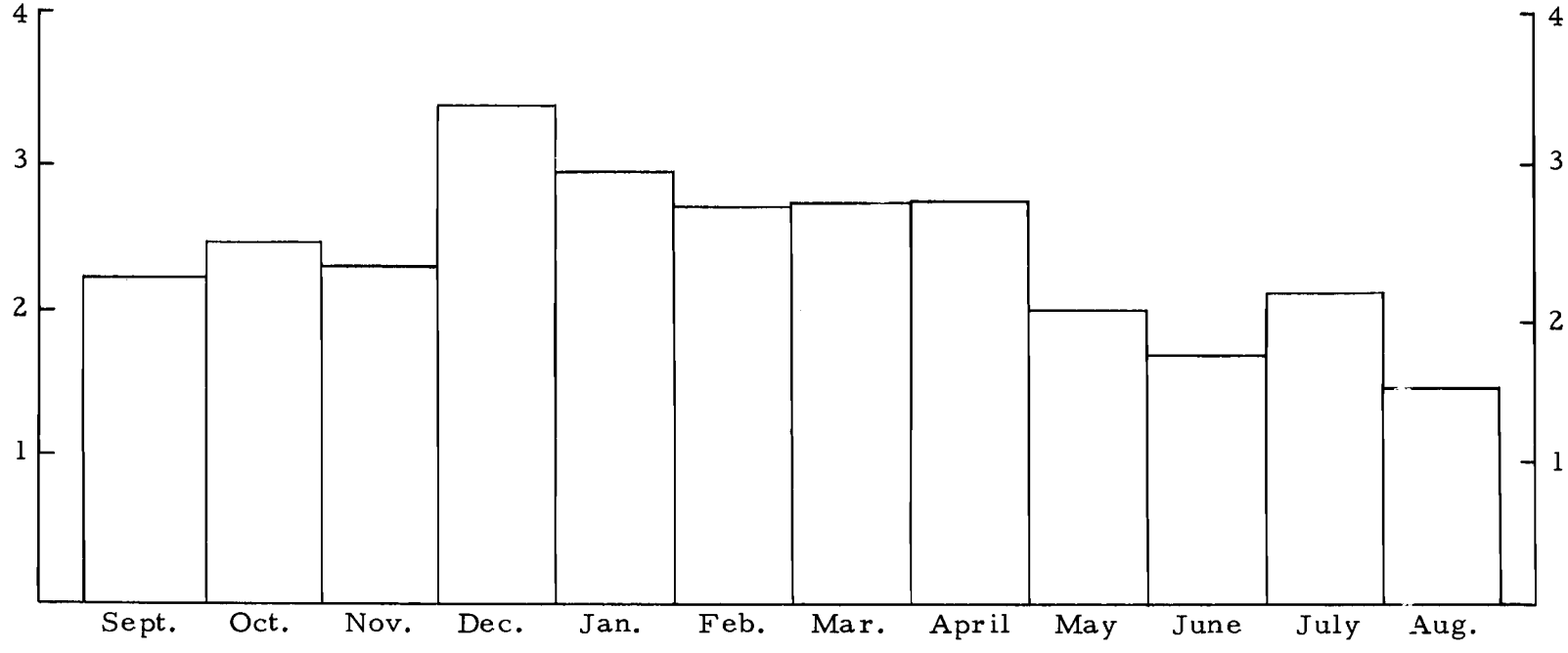

Figure 16. Average monthly deep water wave heights (in meters) at Newport.

data from the Outer Banks beach in North Carolina and found that 72% of the variation in the observed longshore currents could be explained by (1) the angle of wave incidence - 68%, (2) wind velocity - 3%, (3) wave height - 1%, and (4) the beach bed slope - less than 1%. Sonu et al. also applied the regression approach to the field data of Putnam et al. (1949) and found that the angle of wave incidence explained a remarkable 81.6% of the variation.

Harrison (1968), also using a regression scheme, reported a variance reduction of 46% for the angle of wave incidence and 53% for the combined effects of the angle of wave approach and the breaker period. He did not use a term for the prevailing wind. Heights of breakers measured during the study were generally less than 1.3 meters while the angles of wave incidence were less than 16^{o}.

Komar (1969), in studies involving longshore sand transport on California beaches, inferred a direct proportionality between the two most basic theoretical models of longshore currents, namely the longshore component of the wave energy flux reaching the beach and the longshore component of the wave momentum flux, or radiation stress. Longuet-Higgins (1970) mathematically verified Komar's inference and also showed that the longshore current is proportional to U_{max} (sin $\emptyset$), where U_{max} is the maximal orbital velocity of the water particles in the waves and $\emptyset$ is the angle of wave incidence. His equation for longshore velocity at the breaker line is given as

$$\bar{V}_b = 5\pi/8 \quad 2 \left(a B/C \right) \left(gH_b \right) (s \sin \phi_b)$$

where a is a constant of proportionality between breaker height and mean depth (assumed to be about 0.47), B is the tangential bottom stress term (about 0.2), C is a constant coefficient (taken to be 0.007), H_b is the height of the breakers, s is the beach slope, and ϕ_b is the angle of breaker incidence.

Longshore current data for the Yaquina bight study were first grouped as to location and direction of flow versus deep water wave direction (see Table 8). It is apparent that a simple relationship is lacking between the direction of longshore current and angle of wave incidence. On several occasions the current appears to flow opposite to the direction expected from the wave approach.

The theoretical velocity of the currents, as given by Longuet-Higgins (1970), was calculated for each observation. These values versus the observed current are plotted in Figure 17. Again, no strong relationship can be detected. When the observed currents are plotted versus the present hour's wind, however, as in Figure 18, a much better relationship is seen. Therefore a regression analysis was used to predict longshore currents for the beaches at Newport.

Using the same computer program *Step (as described under the Nearshore Currents section) six variables known to be related to longshore currents were selected as independent variables. These were (1) height of the breakers, (2) breaker period, (3) the sine of the

Table 8. Direction frequency of longshore currents for angles of deep water wave approach. (Angles of wave approach are rounded off to the nearest whole multiple of ten degrees.)

Longshore current movement	240° or less	250°	260°	270°	280°	290°	300°	310°	320°	330°	340°
Minnie Street											
North	2	1	1	3	2	9	1		2		
South			1	5	2	5	5	2	7	3	
None					4						
Big Creek											
North	3	2	3	4	7	6			2		
South			2	4	4	5	4	1	4		3
None				1	2	2					

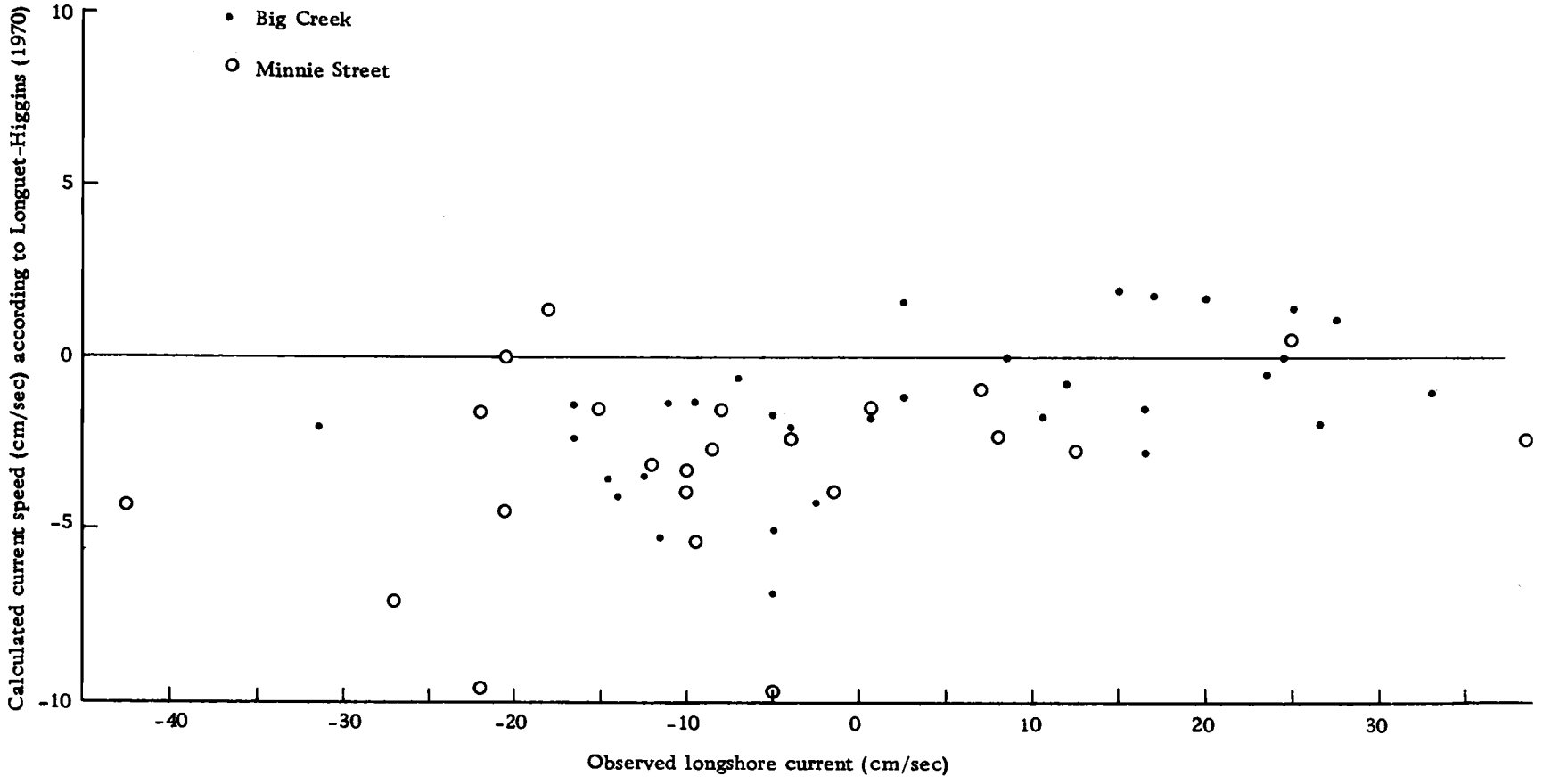

Figure 17. Observed longshore current velocity versus the calculated longshore current velocity according to Longuet-Higgins (1970). Positive values indicate flow to the north.

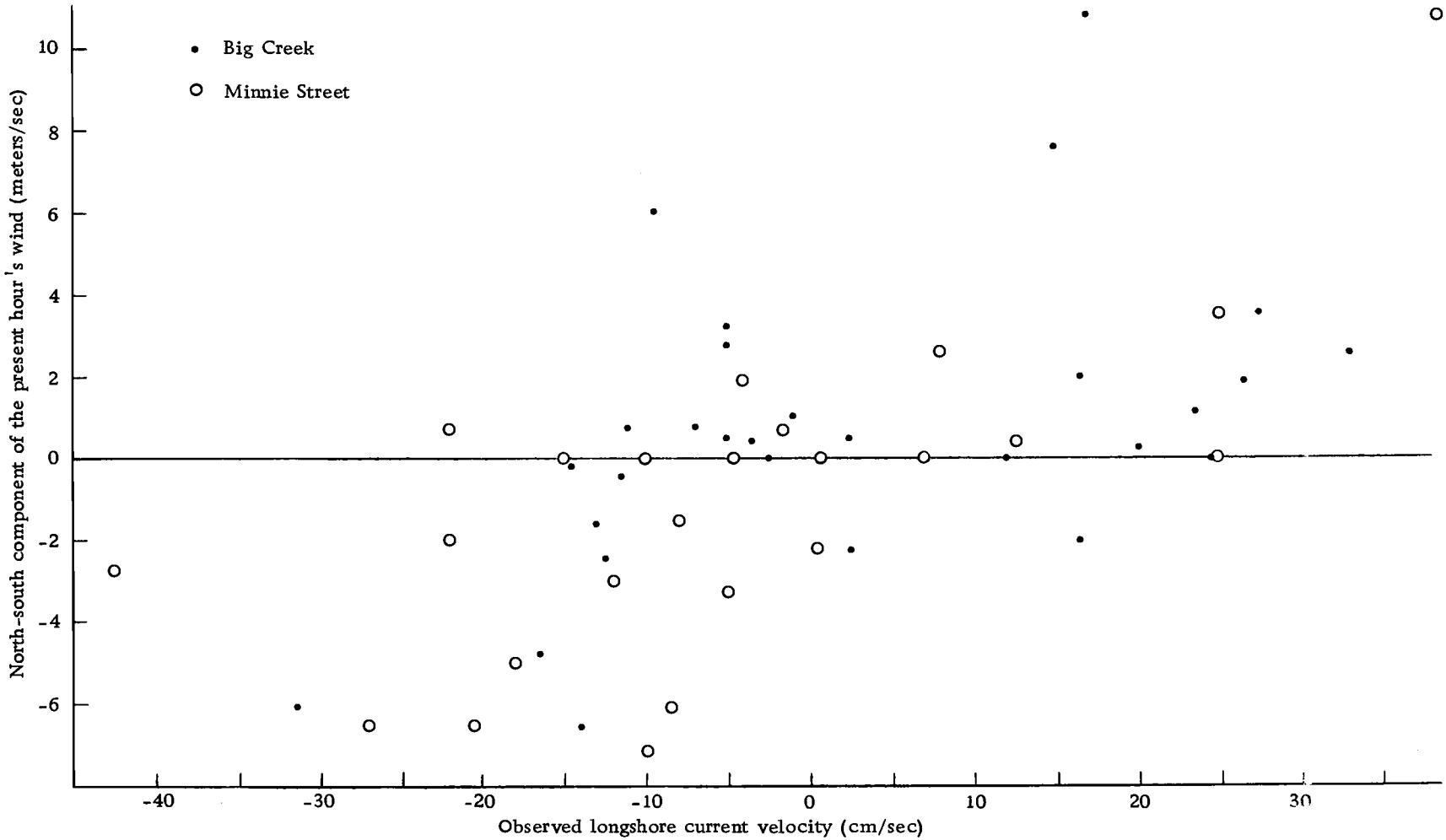

Figure 18. Observed longshore current velocity versus the north-south component of the present hour's wind. Positive values indicate the flow is to the north.

angle of breaker incidence, (4) the north-south tidal component (assuming a standing wave form in the north-south plane), (5) the north-south component of the present hour's wind velocity, and (6) the north-south current component from measurements offshore.

Fifty-three observations of longshore currents with the corresponding six independent variables were analyzed. The observations were recorded at two locations--Big Creek (located near the north end of the beach in the bight) and Minnie Street (near the south end of the beach).

The regression analysis indicated that 51.7% of the variance was "explained" or accounted for by the variables. Of the 51.7%, the wind accounted for 46.2%. The sine of the angle of breaker incidence accounted for 4%, and the remaining 1.7% was due to the height of the breakers, offshore currents, breaker period, and the tidal component. Based on the F level testing for goodness of fit, the wind was significant at the 99% confidence level and the angle of wave incidence at the 95% level. The computed prediction equation for the longshore current velocity is $V = 8.6 + 0.68\ W_{ns} + 47.0\ (\sin \emptyset_b)$, where W_{ns} is the north-south component of the previous hour's wind and $\emptyset_b$ is the angle of breaker incidence. The velocity is predicted to be 8.6 cm/sec towards the north in the absence of wind and waves, indicating a residual drift is present. Referring to Table 8, a breakover point between north and south-flowing currents appears to be

between 280° and 290° rather than the expected 270°. Kulm et al. (1968) also noted that there is a net northerly longshore transport of minerals along the central Oregon coast. Although the relative importance of each variable was established, six variables were considered too many for considering 53 observations. The data were then separated according to location, reducing the number of observations to 30 and 23, respectively. Therefore, only the wind component and the sine of the incident breaker angle were used as independent variables.

The regression analysis then indicated that the wind accounted for 31.7% of the longshore current at Big Creek, significant at the 99% level, while the sine of the incident breaker angle accounted for 3.7% but was not significant at even the 95% level. The prediction equation was computed to be $V = 4.2 + 1.25\ W_{ns} + 0.09 \sin \phi_b$. At the Minnie Street location the wind explained 60.3% of the variance (significant at the 99% level), while the sine of the breaker angle accounted for 5.1% but was not significant at the 95% level. The prediction equation was computed to be $V = 7.9 + 1.79\ W_{ns} + 0.17 \sin \phi_b$.

It is obvious that the combination of the data for the two locations was not justified, as the currents at Minnie Street were nearly twice as predictable as those at Big Creek. However, a positive (flowing to the north) current still exists at both locations throughout the year. Because the

sample size is small, further conslusions drawn from this analysis could be misleading but the significance of the analysis is that the wind is a very important factor in predicting the longshore currents in this location. The incident breaker angle was calculated to be insignificant in accounting for the observed longshore currents at the Newport beaches. Certainly the topography of the location influences the currents as well. Therefore, each local area must be studied individually rather than attempting to use an empirical equation derived from data collected at some other location.

SUMMARY

The water within Yaquina bight appears to be influenced on a large scale by the oceanic seasons which occur off the Oregon coast. The upwelling season (July, August and September) occurs when strong northerly winds produce a net offshore transport of surface waters which are replaced by deeper water flowing on shore. This upwelled water is cold (9°C), saline (33.6‰), and has a low dissolved oxygen content (3.0 to 4.0 ml/l). During the first days of upwelling successive BT traces indicated a vertical velocity of about 20 cm per hour for upwelled water within the bight.

The fall season (October and November) is an intermediate season. The strong northerly winds of the previous season diminish and often reverse in direction. Upwelling becomes less intense and allows a warming of the high salinity water remaining from the previous season.

The winter season (December, January, February and March) is characterized by cool air temperatures, strong southerly winds, heavy precipitation, and a large volume coastal runoff. The surface temperatures are usually cooler than the temperatures at a depth of ten meters. Salinity values are low (30.0 to 32.0‰) and dissolved oxygen content is high (6.5 to 7.0 ml/l). Surface temperatures are generally less than 10°C during most of this season.

Surface temperatures warm rapidly during the spring season (April, May and June). This is also an intermediate season with large variations of temperature and salinity. One brief period of upwelling occurred in May (during this study) but soon ended and warming continued. The warmest temperatures of the year (14.5°C) occurred during this period.

On a smaller scale the waters within Yaquina bight are also influenced by effluent from the pulp mill outfall. The effluent is less dense than the receiving sea water and consequently rises rapidly to the surface. As the effluent rises it also mixes with sea water and as a result, the water over the diffuser pipes and downstream from the diffusers is a mixture of the effluent and sea water. This mixture is generally colder, less saline and less dense than the surrounding surface water. The dissolved oxygen content of the mixture is also lower than the surrounding sea water. Analysis of different effluent-sea water dilutions indicated that the low oxygen content was not due to the effects of the chemical composition of the effluent.

Measurements of current speed and direction were regressed on concurrent measurements of the prevailing winds, waves and tides. The local wind was the dominant current-producing force within the bight. According to the regression analysis, the wind of the hour previous to the time of observation accounted for 56.9% of the variance of the observed currents flowing in the north-south direction and

26.6% of the variance of the east-west flowing currents at the outfall station. The tide accounted for 4.3% of the east-west flow. Other current-producing variables did not contribute to the reduction of variance at the 95% confidence level.

At the Big Creek station the winds during the hour of the current observation accounted for 32.2% of the variance of the north-south currents and 22.2% of the variance of the east-west currents. The currents measured at Yaquina Head and along the north jetty of Yaquina Bay could not be predicted at the 95% confidence level. The currents at these locations appeared to be flowing in response to hydraulic forces encountered from the boundaries imposed by Yaquina Head and the north jetty.

Regression analysis was also used to obtain a predictive equation for longshore currents at two beach locations at Newport. Frequently used equations for predicting longshore current velocities based on the angle of wave incidence and the height of the breakers were inadequate. The north-south component of the wind was the only significant variable (at the 99% confidence level) which could account for the variance in the observed longshore currents. The wind "explained" 60.2% of the variance at the southern section of the beach, but only 31.7% of the variance at the northern end of the beach.

A comparison of the angles observed between the surface current direction and the wind direction indicated that the median

surface current direction was generally to the right of the direction of wind flow at all wind speeds.

The angles between the wind and surface current directions were highly variable but were usually less than 25^{o}. A similar comparison of the angles between the current direction at two meters beneath the surface and the wind direction showed less variability. The median current direction at a depth of two meters was to the left of the direction of wind flow for wind speeds less than 3.5 meters per second and to the right of the wind flow at wind velocities greater than 3.5 meters per second.

The deviation between the surface current direction and the current direction at two meters was apparently related to the season and to the wind speed. At higher wind speeds (above seven meters per second) the angles between the two current directions approached zero. The data did not indicate that the deeper current flowed consistently to the left or the right of the surface current as a function of the wind speed. However, during the upwelling season the current at two meters was observed to flow consistently to the left of the surface current. During the rest of the year the current at two meters flowed to either the left or right of the surface current.

CONCLUSIONS

This study has illustrated the feasibility of a method for collecting nearshore hydrographic data in an area where conventional observation techniques using a boat are difficult throughout much of the year. Aerial observations are hampered only during periods of fog or periods of extensive whitecap coverage accompanying high wind speeds.

The number of ocean outfalls constructed in coastal waters is increasing rapidly. The results of this study indicate that a short preliminary site survey cannot characterize the receiving waters adjacent to a proposed ocean outfall. Observations should be made for at least a period of one year with a frequency of at least once a week. More frequent observations should be collected initially and periodically thereafter to insure that the observational program is providing an adequate sampling interval.

Water circulation is the primary objective of most nearshore studies. The large contribution of the wind to the advection of water warrants an accurate recording of the wind. A reliable and accurate anemometer should be installed near or at the area of observation. Although the wind accounts for much of the water circulation considerable variance is still unexplained. The tides are certainly responsible for some advection of water in the nearshore zone. Installation of moored current meters during favorable weather would

provide a detailed analysis of tidal currents (as well as wave and wind generated currents).

Comparison of surface temperature and salinity obtained from the beach and the temperature and salinity values measured just offshore indicate that monitoring a shore station does not provide data characteristic of the water farther from the beach. A method of remote sampling or periodic sampling by boat is necessary. Future work should include improved aerial techniques for inexpensive and rapid collection of hydrographic data from light aircraft.

BIBLIOGRAPHY

Bretschneider, Charles L. 1967. Estimating wind-driven currents over the continental shelf. Ocean Industry 2(6):45-48.

Brunn, P. 1963. Longshore currents and longshore troughs. Journal of Geophysical Research 68:1065-1078.

Collins, C. A. 1968. Description of measurements of current velocity and temperature over the Oregon continental shelf. July 1965-February 1966. Ph. D. thesis. Oregon State University, Dept. of Oceanography. 153 numb. leaves.

CH_2M, Engineers and Planners. 1965. An engineering report on waste liquor ocean outfall extension. Corvallis, Oregon. 32 p.

Draper, N. R. and H. Smith. 1966. Applied regression analysis. New York, Wiley. 407 p.

Ekman, V. W. 1905. On the influence of the earth's rotation on ocean currents. Arkiv For Matematik, Astronomi ach Fysik 2(11):1-52.

Fleming, R. H. 1938. Tides and tidal currents in the Gulf of Panama. Journal of Marine Research 1:192-206.

Galvin, C. J. 1967. Longshore current velocity: a review of theory and data. Reviews of Geophysics 5:287-304.

Galvin, C. J. and P. S. Eagleson. 1965. Experimental study of longshore currents on a plane beach. Tech. Memo. 10. Army Coastal Engineering Research Center. Washington, D. C. 80 p.

Gonor, J. J. and A. B. Thum. 1970. Sea surface temperature and salinity conditions in 1969 at Agate Beach and Yquina Bay, Oregon. Data report 39. Oregon State University, Dept. of Oceanography. 26 p.

Green, E. J. and D. E. Carritt. 1967. New tables for oxygen saturation of seawater. Journal of Marine Research 25:140-147.

Hall, J. A. 1962. Surf climate at three selected U.S. coastal locales --Atlantic City, N.J.; Hillsboro Inlet, Fla.; Yaquina Bay, Ore. Army Corps of Engineers. p. 24-35.

Harrison, W. 1968. Empirical equation for longshore current velocity. Journal of Geophysical Research 73:6929-2936.

Inman, D. L. and W. H. Quinn. 1951. Currents in the surf zone. Proceedings of the Second Conference on Coastal Engineering. Council on Wave Resesrch, Richmond, Calif. p. 24-36.

James, W. P. 1970. Air photo analysis of water dispersion from ocean outfalls. Ph. D. thesis. Oregon State University, Dept. of Civil Engineering. 141 numb. leaves.

Karwowski, J. 1963. Measurement of sea current by means of drift bottles. International Hydrographic Review 40(2):119-123.

Kinsman, B. 1965. Wind waves: their generation and propagation on the ocean surface. Prentice-Hall, Englewood Cliffs, New Jersey. 676 p.

Komar, P. D. 1969. The longshore transport of sand on beaches. Ph. D. thesis. University of California at San Diego (Scripps Institute of Oceanography). 143 numb. leaves.

Kulm, L. D., K. F. Scheidegger, J. V. Byrne and J. J. Spigai. 1968. A preliminary investigation of the heavy mineral suites of the coastal rivers and beaches of Oregon and northern California. The Ore Bin 30:165-180.

Leipper, D. F. 1955. Sea temperature variations associated with currents in stratified shallow water over an irregular bottom. Journal of Marine Research 14:234-252.

Longuet-Higgins, M. S. 1953. Mass transport in water waves. Philosophical transactions, Royal Society of London, ser. A, vol. 245, no. 903. p. 535-581.

Longuet-Higgins, M. S. 1970. Longshore currents generated by obliquely incident sea waves. Journal of Geophysical Research 75:6778-6801.

Munk, W. H. 1947. A critical wind speed for air-sea boundary processes. Journal of Marine Research 6:203-218.

Pattullo, J. and W. Denner. 1965. Processes affecting seawater characteristics along the Oregon coast. Limnology and Oceanography 10:443-450.

Putnam, J. A., W. H. Munk and M. A. Traylor. 1949. The prediction of longshore currents. Transactions of the American Geophysical Union 30:337-345.

Ralston, A. and H. Wilf. 1962. Mathematical methods for digital computers. New York, Wiley.

Roll, H. U. 1965. Physics of the marine atmosphere. In: International geophysics series, vol. 7. New York, Academic.

Rosenburg, D. H. 1962. Characteristics and distribution of water masses off the Oregon coast. Master's thesis. Oregon State University, Dept. of Oceanography. 45 numb. leaves.

Rossby, C. G. and R. C. Montgomery. 1935. The layer of frictional influence in wind and ocean currents. Papers in Physical Oceanography and Metereology 3(3).

Russel, R. C. H. and J. D. C. Osario. 1958. An experimental investigation of drift profiles in a closed channel. Proceedings of the Sixth Conference of Coastal Engineering, Berkeley, Calif. p. 171-183.

Smith, R. L. 1968. Upwelling. Oceanography and Marine Biology Annual Review 6:11-46.

Sonu, C. J., J. M. McClay and D. S. McArther. 1966. Longshore currents and nearshore topographies. Proceedings of the Tenth Conference on Coastal Engineering, Tokyo, Japan. 1:525-549.

Stokes, G. G. 1880. On the theory of oscillatory waves. Mathematical and physical papers. Vol. 1. Cambridge University Press, Cambridge.

Sverdrup, H. U., M. W. Johnson and R. H. Fleming. 1942. The oceans. New York, Prentice-Hall. 1087 p.

Tollefson, R. 1958. In: CH_2M Engineers and Planners. 1965. An engineering report on waste liquor ocean outfall extension. Corvallis, Oregon. 30 p.

Tomczyak, G. 1964. Investigations with drift cards to determine the influence of the wind on surface currents. Studies on Oceanography 129-139.

Webster, F. 1964. Some perils of measurement from moored ocean buoys. Transactions of the Buoy Technology Symposium 33-48.

Welander, P. 1957. Wind action in a shallow sea: some generalizations of Ekman's theory. Tellus 9:45-52.

Welch, J. G. 1967. A new method of measuring coastal surface currents with markers and dyes dropped from an aircraft. Journal of Marine Research 25:190-197.

Wetz, J. M. 1964. Criteria for judging adequacy of estimation in the reduction of variance according to the F level test. Ph. D. thesis. Madison, University of Wisconsin.